REVIEW

Put a ring on it: application of small aliphatic rings in medicinal chemistry†

Matthias R. Bauer, Paolo Di Fruscia, Simon C. C. Lucas, [iD]
Iacovos N. Michaelides, [iD] Jennifer E. Nelson, [iD]
R. Ian Storer and Benjamin C. Whitehurst [iD] *

Aliphatic three- and four-membered rings including cyclopropanes, cyclobutanes, oxetanes, azetidines and bicyclo[1.1.1]pentanes have been increasingly exploited in medicinal chemistry for their beneficial physicochemical properties and applications as functional group bioisosteres. This review provides a historical perspective and comparative up to date overview of commonly applied small rings, exemplifying key principles with recent literature examples. In addition to describing the merits and advantages of each ring system, potential hazards and liabilities are also illustrated and explained, including any significant chemical or metabolic stability and toxicity risks.

Introduction

Aliphatic 3- and 4-membered ring systems are commonplace within modern medicinal chemistry, frequently exhibiting favourable structural and physicochemical properties which have proven advantageous to molecular optimisation. Such properties generally stem from their intrinsic small size and rigidity, presenting atom-efficient three-dimensional structural scaffolds with defined vectors for pendant functionality.[1] These vectors, combined with potential to make specific polar interactions, provide opportunity for potency and selectivity optimisation through protein-ligand complementarity and molecular pre-organisation. Small rings have been frequently applied to provide new intellectual property space through scaffold hops[2] or, in certain cases, bioisosteric replacements for other ring systems or functional groups,[3–6] sometimes providing improved properties, such as reduced hERG liability, through LogD and pK_a modulation.[7,8] Such rigid compounds can also be less susceptible to oxidative metabolism by promiscuous cytochrome P450 (CYP450) enzymes than more flexible systems, through less favourable recognition and electronics for single electron oxidation. Furthermore, in contrast to planar aromatic rings, small aliphatic rings increase overall fraction of sp^3 carbons (Fsp^3), offering the potential for improved solubility owing to non-planar substituent vectors, disfavouring planar intermolecular crystal-packing interactions.[1,9–11]

Although some small rings such as cyclopropanes[12] have been applied successfully in drug discovery for many years, others such as oxetanes and azetidines have seen increased application and popularity more recently. This in part aligns with increased commercial availability of building blocks containing these rings, plus improved synthetic methods to enable their incorporation into medicinal molecules. Some, such as bicyclo[1.1.1]pentanes and numerous fused and spirocyclic variants of small rings, have only been popularised recently and, although medicinal chemistry applications of these have been limited to date, it is anticipated that more examples will appear in due course, enabling better assessment of their value to drug discovery programs.

In this review, aliphatic small rings which have general application and utility in medicinal chemistry are discussed: cyclopropanes (CyPr), cyclobutanes (CyBu), oxetanes, azetidines and bicyclo[1.1.1]pentanes (BCP; Fig. 1). The attractive medicinal chemistry properties associated with each ring system have been exemplified and potential intrinsic limitations and mitigation strategies are described. As several of these ring systems have been reviewed separately in the past, the focus is largely on recent examples of contemporary medicinal chemistry application. In order to retain focus specifically on broadly useful rings, a few established small rings are not reviewed here. These include aziridines,[13] epoxides,[14] β-lactams,[15–17] squaramides[18,19] and diazirines,[20–22] which have seen specific applications related to their chemical reactivities, but which have largely precluded more general applications in medicinal chemistry: aziridines and epoxides have seen limited application due to their inherent electrophilic reactivity, although several drugs

Discovery Sciences, BioPharmaceuticals R&D, AstraZeneca, Cambridge, UK.
E-mail: ben.whitehurst@astrazeneca.com

† All authors contributed to writing the manuscript.
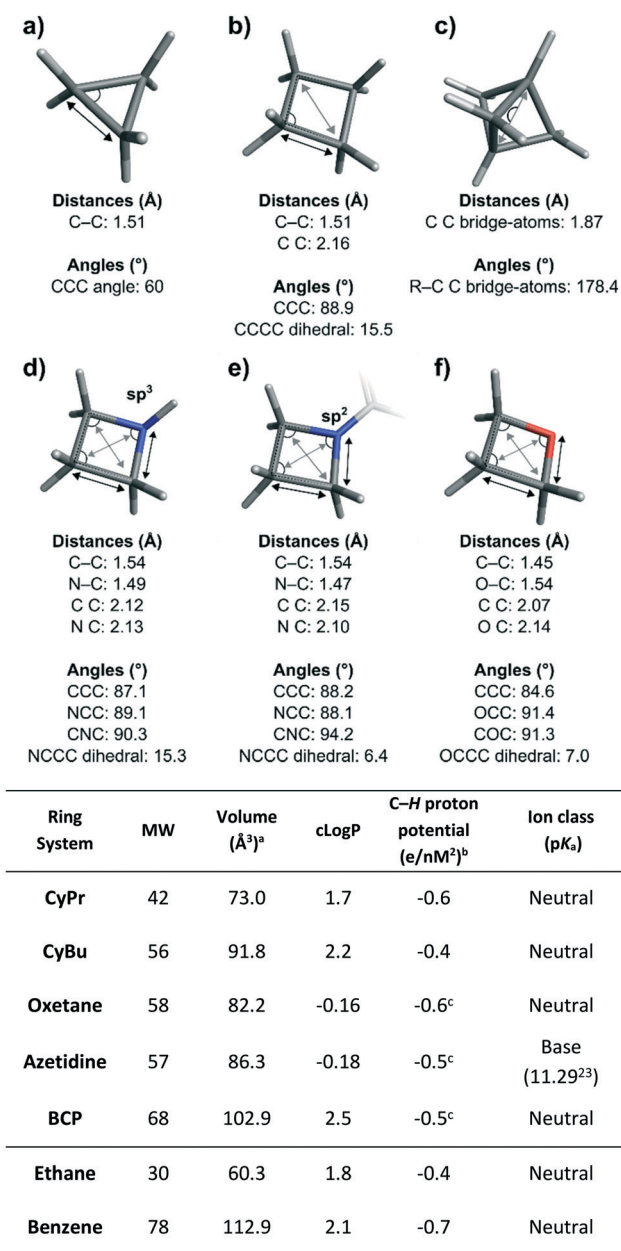
Fig. 1 Top: Median values for key structural parameters of the small rings featured in this review. a) Cyclopropane. b) Cyclobutane. c) Bicyclo[1.1.1]pentane. d) Azetidine with sp^3 hybridised nitrogen atom. e) Azetidine with sp^2 hybridised nitrogen atom. f) Oxetane. Ring systems are depicted without substituents except for the azetidine with sp^2 nitrogen. Bonded (A–A) and non-bonded atom distances (A A) are highlighted respectively with black and grey arrows and non-redundant angles are shown as circular segments. Statistics were generated via analysis of data from the Cambridge Structural Database, the Protein Data Bank, and in-house X-ray data using RDkit[24] for substructure matching and computation of geometric values, and Spotfire for statistical analysis.[25] The analysis included spirocyclic derivatives but not fused and bridged systems (with the exception of bicyclo[1.1.1]pentanes). Bottom: Structural and physicochemical features of the ring systems featured in this review. Benzene and ethane are included for comparison. [a]Van der Waals volume. [b]Measured using COSMO surfaces.[26,27] [c]Most polarized protons (C–H adjacent to heteroatom for oxetane and azetidine; bridgehead C–H for BCP).

including thiotepa, mitomycin, eplerenone, fosfomycin, scopolamine and tiotropium do contain these rings, often as covalent antibiotics or alkylating agents; β-lactams are also synonymous with antibiotics, owing to the ability to form covalent adducts with penicillin binding proteins resulting in inhibition of bacterial cell wall biosynthesis;[15–17] diazirines have been applied widely as photoaffinity reagents for covalent cross-linking to proteins upon ultraviolet photoactivation.[20–22]

Cyclopropanes

Introduction

Cyclopropane (CyPr) rings are the most ubiquitous small ring system in medicinal chemistry. They appear in >60 marketed pharmaceutical agents with a wide variety of indications from Oncology to HIV.[12] In 2019, CyPr rings featured in 642 patent applications, and have consistently been the most frequently used small ring in the patent literature (Fig. 2).[28] The reasons for its prevalence are many-fold but primarily hinge upon the unique structure and physicochemical properties of the ring.

Structural features and physicochemical properties of cyclopropanes

The unique characteristics of the CyPr group arise from the 60° internal angle (Fig. 1). This creates a planar, rigid structure with well-defined exit vectors and significant ring strain (27.5 kcal mol^{-1}).[29] The internal C–C bonds have more p-character and, as such, they are often considered pseudo double bonds, despite retaining a bond length (1.51 Å) closer to an aliphatic C–C bond. As a further consequence of the ring strain, the C–H bonds have more s-character and are shorter, stronger and more polarised than conventional C–H bonds (see table in Fig. 1). On average the CyPr ring is 0.2 and 0.5 log units less lipophilic than iPr groups and phenyl rings respectively, making it an attractive substituent for medicinal chemistry applications.[30]

Medicinal chemistry applications of cyclopropanes

CyPr groups have found extensive use in medicinal chemistry and have been employed to increase potency, provide conformational stability, and improve pharmacokinetics (PK) and solubility.[12] They are frequently used as isosteres for small alkyl groups (e.g. Me and iPr), aromatic rings and alkenes. The use of CyPr in marketed drugs has been extensively reviewed[12] and this section will focus on contemporary applications and limitations of their use.

Isopropyl isostere. The E3 ligase Von Hippel–Lindau (VHL) is an important target in medicinal chemistry due to its role in protein degradation. Bifunctional ligands containing a VHL binding warhead are able to harness this ligase to promote ubiquitination and subsequent proteasomal degradation of target proteins.[31,32] Due to the increased size requirements for a bifunctional ligand, efficient warheads for the E3 ligases such as VHL will be crucial to their success.
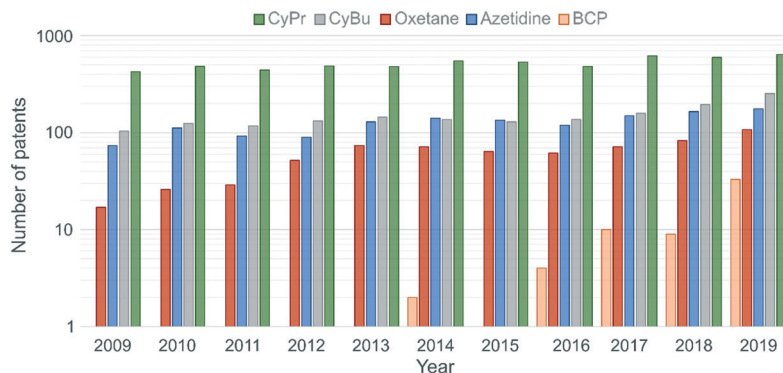
Fig. 2 Number of drug substance patents containing CyPr, CyBu, oxetane, azetidine and BCP substructures filed between 2009 and 2019.[28] β-Lactones and β-lactams were excluded from the analysis.

Ciulli *et al.* recently showed that a small lipophilic CyPr was an optimal substituent in a series of peptide mimetics.[33] Switching from iPr **1** to CyPr **2** gave a 9-fold increase in potency against the target which the authors attributed to the binding pocket being more accommodating to the smaller, constrained CyPr analogue (Fig. 3). The CyPr was also less lipophilic, an important consideration when working in 'beyond rule-of-5' space.[34]

This VHL warhead was subsequently used by the same authors in the development of BAF degraders where the CyPr group formed a crucial part of the ternary complex interface.[35] The iPr to CyPr change is one that is often employed by medicinal chemists during systematic structure–activity relationship (SAR) exploration[36] and there are also numerous examples where the CyPr is detrimental to affinity.[37,38] Additionally, this change is often exploited to improve metabolic stability, due to the shorter, stronger bonds in CyPr compared to iPr,[12] however, this was not discussed during the optimisation of VHL ligands.

Aromatic ring replacement. The CyPr group has long been recognised as a viable replacement for aromatic rings that can improve the physicochemical properties of the molecule through increased Fsp.[3] Recently, scientists at Genentech reported **3** as a noncovalent inhibitor of Bruton's tyrosine kinase (BTK) (Fig. 4).[39] However, there was concern that the

presence of a 2,5-diaminopyridine represented a structural hazard and could cause drug induced liver injury through *in vivo* bioactivation.[40] Replacement of the aromatic ring with an amide F-CyPr **4** maintained potency despite a significant reduction in molecular weight.[41] X-ray crystallography revealed that the carbonyl oxygen overlapped with the pyridine nitrogen and that the polarised α-carbonyl CyPr
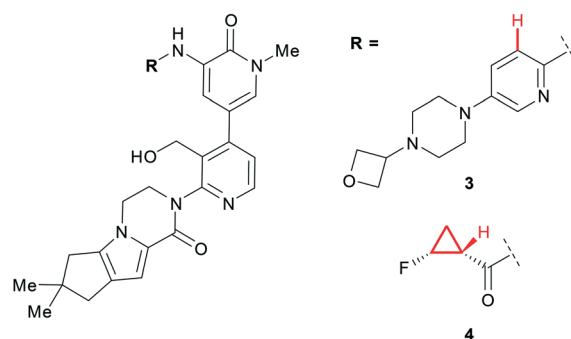
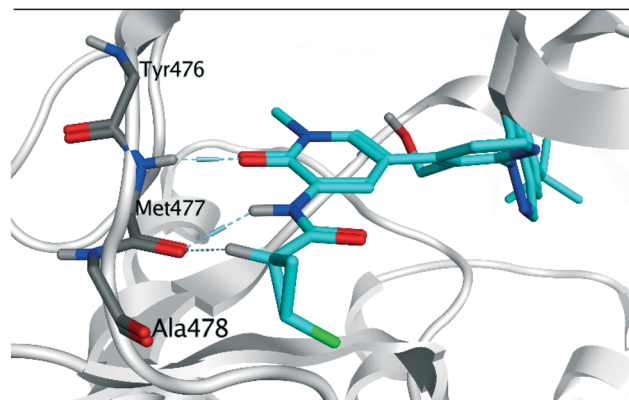| Cmpd	BTK IC$_{50}$ (nM)	LogD$_{7.4}$
3	2.3	1.6
4	2.3	2.3

Fig. 4 Top: Optimisation of BTK inhibitors by replacement of a 2,5-diaminopyridine, a potential structural hazard.[41] Bottom: Close-up view of **4** (cyan) bound to BTK (PDB code: 6XE4), highlighting hydrogen bonding interactions (pale blue dashed lines) with the hinge (Met477), including nonclassical hydrogen bond with the polarised CyPr proton.[41]
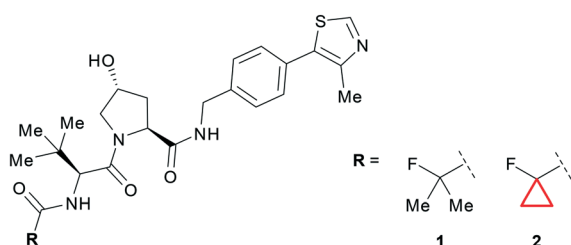
Cmpd	VHL K$_d$ ITC^a (nM)	cLogP
1	770	3.0
2	90	2.7

Fig. 3 CyPr as an iPr isostere in the optimisation of VHL ligands.[33] ^{a}Isothermal titration calorimetry.

proton makes a hydrogen bond to a kinase hinge carbonyl (previously made by the pyridine C–H; highlighted in Fig. 4).

Further optimisation of the cyclopenta[4,5]pyrrolo[1,2-*a*] piperazinone moiety present in **4** resulted in a lead series, however further progress was halted due to hERG activity.[41]

Conformational stability. The ability of the CyPr group to constrain aliphatic systems is well documented and has been used in the development of drugs such as lemborexant.[42] A CyPr ring was also used to constrain a benzyl group during the development of a series of phosphodiesterase 2 (PDE2) inhibitors.[43] Extending out from a fragment hit into a lipophilic pocket with a *para*-CF$_3$ benzyl group gave lead compound **5** with 2.34 μM affinity for PDE2 (Fig. 5).

Initial attempts to improve the potency identified methyl substituted **6** with a 10-fold increase in PDE2 affinity over **5**. Molecular modelling suggested that a CyPr group would stabilise the bioactive conformation by allowing it to adopt the preferred torsion angle with the distal phenyl ring. This led to a 50-fold increase in potency and a much improved lipophilic ligand efficiency (LLE)[45,46] for CyPr **7**, whilst maintaining the physicochemical properties of the series. A close analogue of **7**, containing the CyPr, had suitable PK for an *in vivo* tool.

Morpholine isostere. The π-character of the CyPr ring was recently exploited by scientists at GSK to conformationally restrict the free rotation of a tetrahydropyran (THP) ring as an isosteric replacement for morpholines.[47] The 4-(pyrimidin-4-yl)morpholine motif is a privileged structure in targeting the phosphoinositide 3-kinase (PI3K)-AKT-mammalian target of rapamycin (mTOR) pathway that appears in multiple patents and papers.[48–50] Crucial to its success is the co-planarity afforded by an overlap of the nitrogen lone-pair and the aromatic system, with the morpholine oxygen acting as a hinge binder by hydrogen bonding to Val882. The authors proposed that a CyPr-THP would maintain the desired co-planarity whilst positioning the oxygen to form the key hydrogen bond. They demonstrated that this could be achieved with compound **9** which maintained potency (pIC$_{50}$ = 8.6), with no detrimental effect on the physicochemical properties *vs.* the parent methyl morpholine **8** (Fig. 6). However, it should be noted
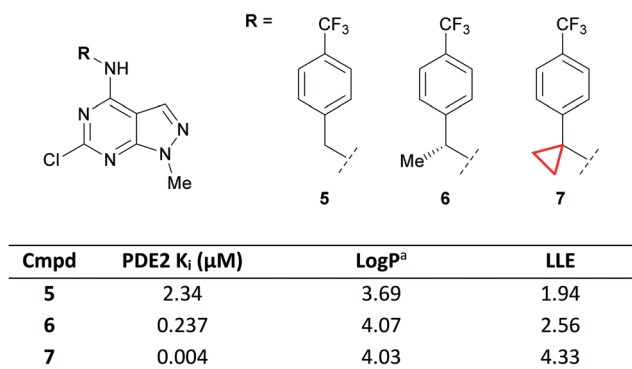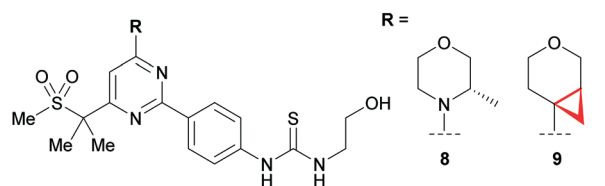

Cmpd	mTOR pIC$_{50}$	LogP[a]	Solubility[b] (μg/mL)
8	8.4	3.6	151
9	8.6	3.9	173

Fig. 6 CyPr THP as a morpholine isostere in a PI3K–mTOR inhibitor.[47] [a]Log*P* = measured ChromLog*P*.[51] [b]Kinetic solubility measured at pH 7.4.

that raised microsomal and hepatocyte clearance was observed for two additional CyPr-THP exemplars relative to their methyl morpholine matched pair (data not shown).

Alkene isostere. The stabilising effect of the CyPr group was recently used by a group at Pfizer in the development of CyPr-chromane γ-secretase inhibitors as agents that can reduce amyloid plaques (*e.g.* Aβ42), a pathology implicated in Alzheimer's Disease.[52] The authors were initially looking for replacements for a naphthyl group and identified chromene **10** which showed potent reduction of Aβ42 *in vitro* but suffered from high clearance (Fig. 7). Metabolic identification (MetID) studies showed that this was primarily driven by CYP-mediated oxidation of the methylene between the alkene and chromene O atom. Introduction of the CyPr **11** improved potency through stabilisation of the bioactive conformation, and reduced metabolism through removal of the allylic methylene. Further work identified **12** which gave better brain exposure through increased lipophilicity. This compound displayed excellent tolerability up to 300 mg kg^{-1} in a rat dose escalation study and showed 40% reduction of brain Aβ42 after 4 hours when dosed orally at 10 mg kg^{-1}.

***t*-Butyl isostere.** Due to the 3D characteristics of CyPr and the ability to break up crystal packing, CyPr rings are often

Cmpd	PDE2 K$_i$ (μM)	LogP[a]	LLE
5	2.34	3.69	1.94
6	0.237	4.07	2.56
7	0.004	4.03	4.33

Fig. 5 Optimisation of PDE2 ligands *via* conformational stabilisation.[43] [a]Log*P* = Alog*P*$_{98}$.[44]
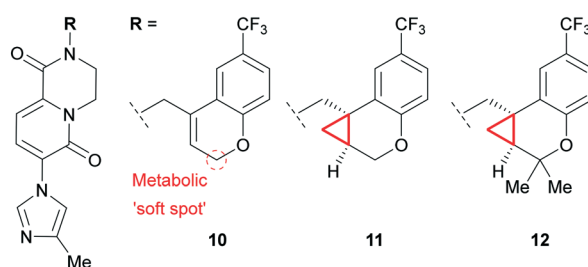
Cmpd	Aβ42 IC$_{50}$ (nM)	cLogP	HLM[a] Cl$_{int, app}$ (μL/min/mg protein)
10	30	2.4	108
11	5.6	2.4	37.9
12	4.9	3.2	34.5

Fig. 7 Exploration of CyPr as an alkene isostere.[52] [a]Human liver microsomes.
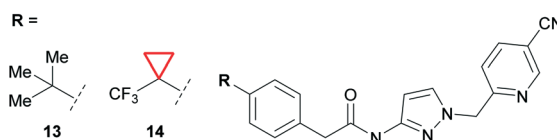
employed to improve solubility. Recently, a team from Idorsia Pharmaceuticals Ltd reported the development of selective T-type calcium channel (TTCC) blockers for the treatment of epilepsies.[53] During their drug discovery program **13** was identified as a potent TTCC blocker, but it was limited by poor solubility and low brain exposure (Fig. 8). The authors showed that switching to a CF$_3$–CyPr (**14**) improved solubility with little effect on lipophilicity. This was important as previous SAR showed that more polar compounds become P-gp substrates with limited CNS penetration. CyPr **14** was thus identified as a suitable drug candidate to treat epilepsy and has since entered clinical trials.

The CF$_3$–CyPr had previously been reported by researchers at Novartis as a metabolically stable *t*-Bu isostere.[54] In the above example, metabolic stability was good for both **13** and **14** and the authors state that the change was part of the systematic SAR exploration.

Liabilities of cyclopropanes

Cyclopropylamine as a structural alert. As discussed previously, CyPr groups are often introduced to address metabolic instability of *i*Pr groups. However, cyclopropylamines may be substrates for both monoamine oxidase (MAO) and CYP450 oxidation, which can result in the formation of reactive metabolites.[55] The bioactivation is understood to either proceed through single electron transfer from the nitrogen to form a radical cation, which can then undergo ring opening to form a reactive radical and iminium ion, or through hydroxylation of the CyPr carbon adjacent to the amine and subsequent dehydration to form an iminium ion (Fig. 9a).[56] Time-dependant inhibition of CYP450s is often observed for compounds with this chemotype as the generated reactive intermediate can inhibit the metabolising enzyme.[57,58]

Trovafloxacin **15** (Fig. 9b) is a broad spectrum antibiotic which was withdrawn from the market due to hepatotoxicity.[59] It is believed that oxidation of the cyclopropylamine and subsequent breakdown into a reactive metabolite is the most likely mechanism of action for the
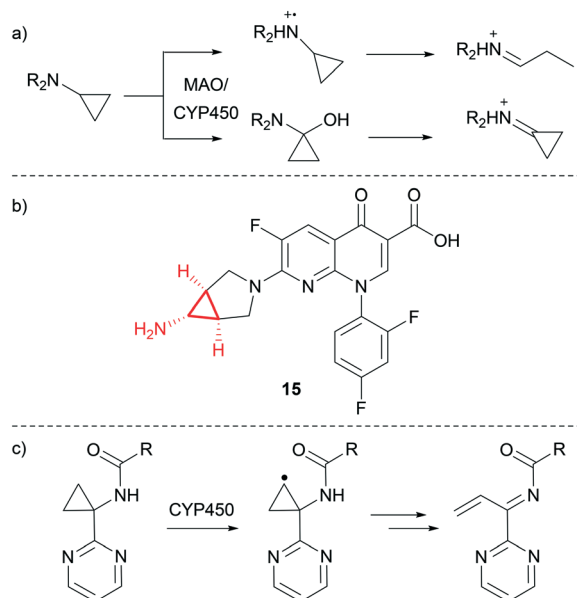

Fig. 9 a) Mechanisms of reactive metabolite formation from CyPr amines.[56] b) Trovafloxacin.[59] c) CYP450-mediated oxidation of a cyclopropylamine β-carbon.[60,61]

observed toxicity, although the exact route of bioactivation is unknown.

In another recent example, researchers at BMS reported a series of Hepatitis C virus NS5B inhibitors where CYP450-mediated oxidation of a cyclopropylamine β-carbon led to the formation of a reactive intermediate (Fig. 9c).[60,61] In this case, switching to the *gem*-dimethyl stopped the formation of reactive intermediates whilst maintaining potency.

There have also been instances where the chemical stability of cyclopropylamines has been problematic. GSK2879552 (**16**) is a lysine-specific demethylase inhibitor currently undergoing clinical trials.[62] It was revealed that this compound was unstable at high pH and that complete degradation occurred in 0.1 M NaOH after just 2 hours at 80 °C. After a thorough mechanistic study the authors proposed that at higher pH the basic CyPr-amine is uncharged and can react through the nitrogen lone pair *via* ring opening of the CyPr, leading to chemical degradation (Fig. 10). They claimed that the phenyl ring stabilises the transition state and that

Fig. 8 Improving the solubility of TTCC blockers using CyPr.[53] [a]Log D = AZ log D, calculated Log D at pH 7.4. [b]Solubility measured at pH 7.0. [c]Unbound concentration in the brain. Wistar rats were dosed orally with 10 mg kg^{-1} of **13** and **14**.

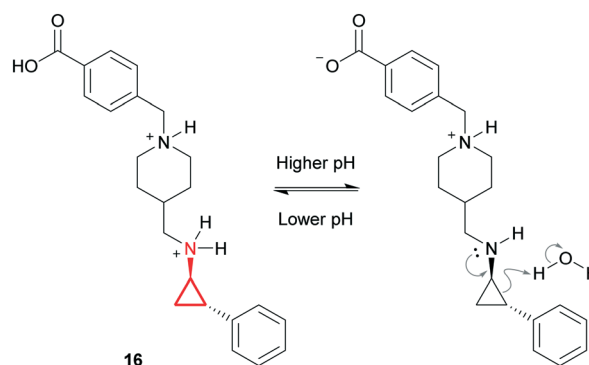| Cmpd	Ca$_v$3.1 IC$_{50}$ (nM)	LogD[a]	Solubility[b] (mg/L)	C$_{u,brain}$[c] (nM)
13	2.8	2.90	<1	6.1
14	6.4	2.78	5	29

Fig. 10 Chemical degradation of GSK2879552 (**16**).[62]

the driving force is the release of the strain energy. However, it is not clear why stability is such an issue in this example when the pharmacophore appears in several marketed drugs (*e.g.* tranylcypromine). Ultimately a stable formulation was identified through careful salt selection. Their strategy was to decrease the solubility of the complex whilst maintaining a saturated aqueous pH <5. This resulted in the identification of a napadisylate (dihydrate) formulation which had suitable stability for development.

Cyclopropyl carboxylic acid as a structural alert. Compounds which contain a fragment capable of forming CyPr carboxylic acid *in vivo* should also be considered a structural alert because they can form carnitine conjugates.[63] Carnitine is a small molecule involved in energy metabolism that transports long-chain fatty acids into mitochondria. Inhibition of this process through the formation of CyPr carnitine conjugates can lead to a toxic build-up of fatty acids or carnitine depletion. A phase 1 trial of the anxiolytic panadiplon (**17**) was recently paused due to hepatotoxicity.[64] It is thought that metabolism generates CyPr carboxylic acid **18** and subsequent conjugation to carnitine conjugate **19** drives the observed toxicity (Fig. 11). Carnitine depletion only presents after chronic treatment with high doses and could potentially be mitigated by taking carnitine supplements. However, during optimisation, MetID studies can be used to identify whether formation of CyPr carboxylic acid is a major metabolic pathway.

Outlook

The CyPr group is a stalwart of medicinal chemistry and its use has arguably become more creative in recent years. Despite potential risks, such as reactive metabolite formation, the CyPr group will continue to be used extensively because of its unique properties and ability to improve potency, provide conformational stability, reduce metabolism and increase solubility.

Cyclobutanes

Introduction

Numerous medicinal chemistry manuscripts now report biologically active cyclobutane (CyBu)-containing compounds with improved activi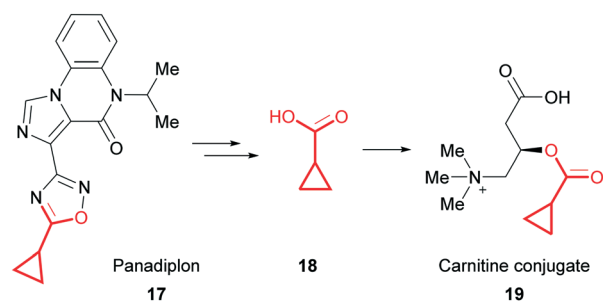ty and properties compared to their acyclic counterparts. In addition, the CyBu motif is recurrent in patents, with consistent application over the past decade (Fig. 2). Furthermore, in the last few decades the use of CyBu derivatives as molecular building blocks in organic synthesis has flourished, and many reliable preparative methods have been reported.[65–67] The increased popularity of this cycloalkane ring system in organic synthesis, coupled with its unique structural and physicochemical features has boosted its broad use in medicinal chemistry. To date, 9 FDA-approved drugs containing a CyBu group have been marketed, spanning a wide range of indications.[28]

Structural features and physicochemical properties of cyclobutanes

In contrast to CyPr, CyBu is not planar but puckered, relieving eclipsing 1,2-interactions: the median puckering angle for CyBu is 15.5° (Fig. 1). In addition, the CyBu median CCC bond angle of 88.9° is a significant deviation from the ideal tetrahedral bond angle for carbon (109.5°), resulting in considerable ring strain compared to its larger homologues cyclopentane and cyclohexane (26, 6 and 0 kcal mol^{-1} respectively).[68] CyBu groups are often used to rigidify linear alkyl chains linking two pendant functionalities; the median C C nonbonding distance of CyBu is 2.16 Å.

Medicinal chemistry applications of cyclobutanes

The CyBu ring system is often employed as a standalone substituent, for example as a mono-substituted pendant group or a 1,1-disubstituted *gem*-dimethyl isostere to maximise Van der Waals contacts with a target protein. *Cis* and *trans* 1,3-disubstituted CyBu rings have use as bridging motifs, restricting free rotation of an aliphatic chain. Such application to increase molecular rigidity has been shown to enhance binding affinity (minimising the entropic penalty of protein–ligand binding) and cellular permeability.[69]

In light of the small and compact 3-dimensional character of the CyBu group, in combination with its steric and electrostatic properties, incorporation of this carbocyclic small ring into drug molecules can often lead to improved physicochemical and ADME (absorption, distribution, metabolism, excretion) properties, such as solubility and metabolic stability.[70] This section reviews successful medicinal chemistry application of CyBu over the past decade.

Aliphatic chain restriction (with extension). CyBu rings can dramatically impact candidate selection, as demonstrated by Kono *et al.* during the development of novel retinoic acid-related orphan receptor γt (RORγt) inverse agonists.[71] Potent RORγt inverse agonistic activity was demonstrated, achieving excellent selectivity against other ROR isoforms and nuclear receptors, as well as a suitable PK profile. Here, the authors introduced a *cis* 1,3-disubstituted CyBu ring into lead molecule **20** as a replacement to an unconstrained aliphatic linker towards a pendant carboxylate (itself required to modulate PK properties).[72] Conformationally constrained
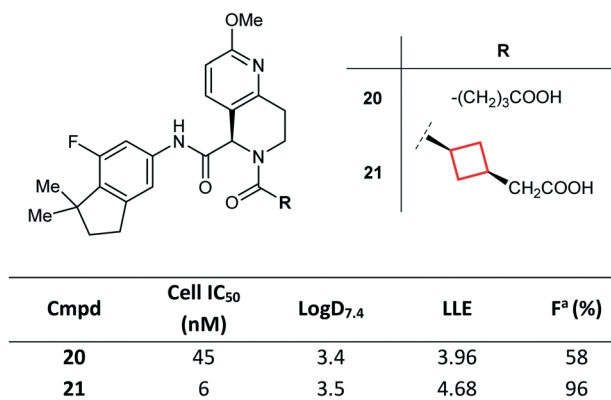

Fig. 11 Formation of a CyPr carnitine conjugate from panadiplon (**17**).[64]

Fig. 12 Optimisation of RORγt inverse agonists *via* conformational rigidification of the acid tether with a CyBu group.[71] [a]Fraction of dose reaching systemic circulation (bioavailability). Mice were dosed orally with 10 mg kg^{-1} of **20** and **21**.

Cmpd	Cell IC$_{50}$ (nM)	LogD$_{7.4}$	LLE	F[a] (%)
20	45	3.4	3.96	58
21	6	3.5	4.68	96

molecule **21** was found to have improved potency (by stabilisation of the biologically relevant conformation) and optimal oral bioavailability and plasma exposure (Fig. 12). Of note, the *trans*-isomer was less potent than *cis*-isomer **21** (data not shown). On the basis of its potent *in vivo* efficacy and favourable preclinical PK profile, compound **21** was ultimately selected as a clinical candidate.

Aliphatic chain restriction (with contraction). Replacement of a flexible alkyl chain with a rigid, constrained CyBu group may enhance the metabolic stability and PK profiles of molecules, as demonstrated by Zhao *et al.*[73] Compound **22**, a previously reported inhibitor of the MDM2 (murine double minute 2 homolog)-p53 interaction, was found to suffer from low metabolic stability, and MetID studies revealed the 1,2-diol side chain as the major metabolic soft spot. By conformationally constraining the carbinol side chain, consequently reducing the number of rotatable bonds in the molecule, the authors were able to identify CyBu **23** (MI-888) as a potent MDM2 inhibitor with improved metabolic
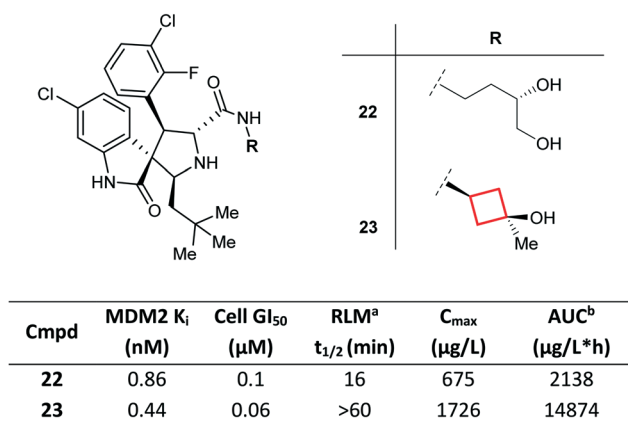
stability in rat liver microsomes, superior oral PK profile (in particular, systemic exposure) and enhanced *in vivo* efficacy compared to **22** (Fig. 13). Remarkably, compound **23** was shown to achieve rapid, complete, and durable tumour regression in two types of tumour xenograft models.

Ring contraction. Another example that shows how a CyBu core played a paramount role in the development of a drug candidate is represented by sulfonamide **24** (PF-04965842): a selective JAK1 agent for the treatment of autoimmune diseases, developed from tofacitinib (**25**; Fig. 14).[74] The significant JAK2 activity of tofacitinib may cause haematotoxicity, such as anaemia and thrombocytopenia, thus compounds with a JAK1-selective profile were deemed highly desirable. Replacement of the 3-aminopiperidine in tofacitinib with a *cis*-1,3-cyclobutyldiamine delivered a JAK1-selective chemotype. In particular, exemplar **24** was found to be a potent and selective JAK1 inhibitor with good physicochemical properties.

Gem-**Dimethyl replacement.** The CyBu ring is often used in medicinal chemistry as an isostere of the *gem*-dimethyl group. In the pursuit of selective cannabinoid receptor 1 (CB1) agonists, a variety of conformationally modified side chains in tricyclic framework **26** were explored. Whilst *gem*-dimethyl **26** was unselective *vs.* CB2, replacement with a CyBu group in **27** led to enhanced potency and a 16-fold selectivity margin (Fig. 15).[75]

Chain branching. Introduction of a CyBu group may be advantageous in improving stability of metabolically labile aliphatic chains and in improving the overall binding affinity by filling small neighbouring hydrophobic pockets in the target protein. Imidazo[4,5-*b*]pyridine derivative **28** was optimised to improve both pan-AKT (protein kinase B) activity and the overall profile of the class. The optimisation campaign led to the discovery of CyBu-containing lead molecule ARQ 092 (**29**), which demonstrated high enzymatic potency against AKT1, AKT2 and AKT3, as well as potent cellular inhibition of AKT activation and the phosphorylation of the downstream target PRAS40 (Fig. 16).[76] Compound **29** was also found to have higher metabolic stability in human

Fig. 13 Optimisation of inhibitors of the MDM2–p53 interaction *via* conformational rigidification of the carbinol side chain with a CyBu group.[73] [a]Rat liver microsomes. [b]Area under the plasma concentration time curve. Rats were dosed orally with 25 mg kg^{-1} of **22** and **23**.

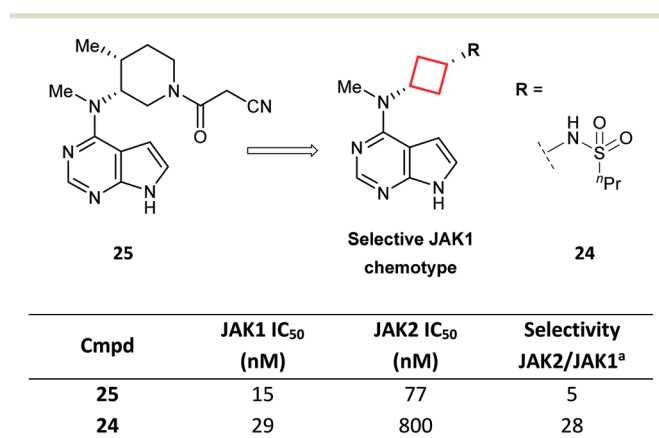| Cmpd	MDM2 K$_i$ (nM)	Cell GI$_{50}$ (μM)	RLM[a] t$_{1/2}$ (min)	C$_{max}$ (μg/L)	AUC[b] (μg/L*h)
22	0.86	0.1	16	675	2138
23	0.44	0.06	>60	1726	14874

Fig. 14 Optimisation of selective JAK1 inhibitors *via* ring contraction of a piperidyl ring to a CyBu core.[74] [a]Ratio of IC$_{50}$ for JAK2 *vs.* JAK1.

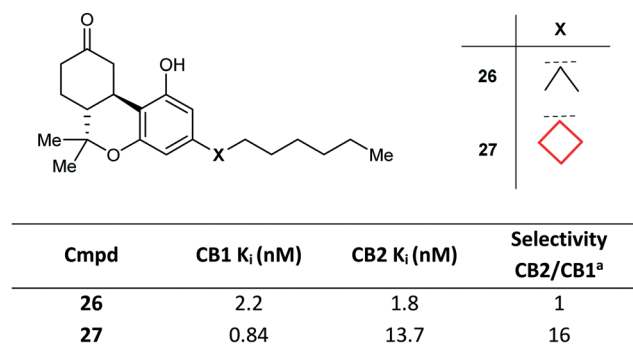| Cmpd	JAK1 IC$_{50}$ (nM)	JAK2 IC$_{50}$ (nM)	Selectivity JAK2/JAK1[a]
25	15	77	5
24	29	800	28

Fig. 15 Development of cannabinoid receptor 1 (CB1) agonists *via* *gem*-dimethyl replacement with a CyBu group.[75] [a]Ratio of binding affinities for CB2 *vs.* CB1.
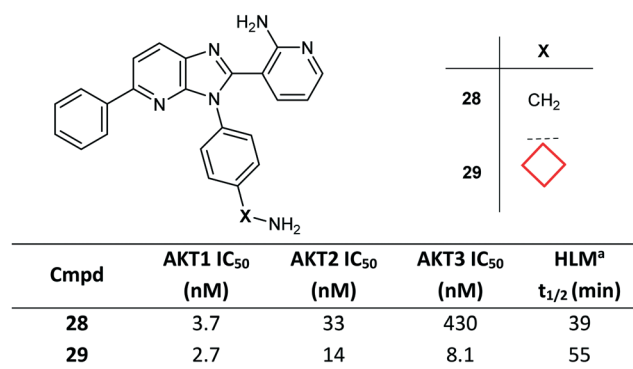
Cmpd	CB1 K_i (nM)	CB2 K_i (nM)	Selectivity CB2/CB1[a]
26	2.2	1.8	1
27	0.84	13.7	16

Cmpd	AKT1 IC_{50} (nM)	AKT2 IC_{50} (nM)	AKT3 IC_{50} (nM)	HLM[a] $t_{1/2}$ (min)
28	3.7	33	430	39
29	2.7	14	8.1	55

Fig. 16 Optimisation of AKT inhibitors *via* side chain branching with a CyBu group.[76] [a]Human liver microsomal stability at 1 μM test compound.

liver microsomes preparations compared to parent molecule **28**. A co-crystal structure of compound **29**, bound to full-length AKT1, confirmed the allosteric mode of inhibition of this chemical class and the role in affinity gains of the CyBu group, placed in a hydrophobic cleft.

Liabilities associated with cyclobutanes

Metabolism of CyBu substructures. Whilst the CyBu group can be effectively employed to enhance the metabolic profile of drug molecules, success depends on the overall architecture and favourable physicochemical properties of the designed compounds. A CyPr to CyBu switch is a commonplace medicinal chemistry transformation when investigating SAR, often resulting in potency gains if lipophilic contacts are improved. However, Åstrand *et al.* demonstrated that CyBu-fentanyl **30** was less metabolically stable than the CyPr derivative **31** when incubated with human hepatocytes (Fig. 17). MetID studies revealed that *N*-dealkylation was the predominant metabolic transformation for both **30** and **31**, to give corresponding piperidines **32** and **33**. In addition, oxidation of the CyBu ring to give **34** was a major metabolite for **30**, whilst oxidation of the CyPr ring in **31** was not observed.[77] Interestingly, cleavage
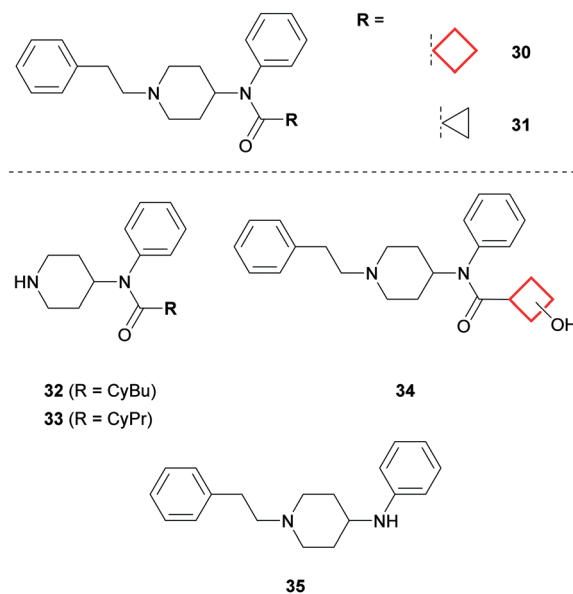

Fig. 17 MetID studies on CyBu-fentanyl (**30**) and CyPr-fentanyl (**31**).[77]

of the CyBu amide bond was another significant metabolite for **30** to give **35**, whereas the corresponding biotransformation was not observed for CyPr **31**. Indeed, it is possible that the resulting CyBu carboxylic acid metabolite may also be capable of forming carnitine conjugates *in vivo*, as for CyPr acid metabolites (*vide supra*).[63,78]

Synthetic tractability. Whilst developing novel methods towards the syntheses of CyBu rings has gained increasing attention (particularly through photocycloaddition routes,[67] or in the context of specific, complex natural products[79]), CyBu synthetic chemistry still remains largely underdeveloped. In particular, the ability to make select point changes to this ring system presents a large challenge, which has restricting implications for the structure-based and physicochemical property-based design of CyBu-containing molecules in medicinal chemistry.

Outlook

The CyBu ring is an important small ring in the medicinal chemistry toolbox, providing a small lipophilic group to enhance contacts with a target protein, or a structurally rigid scaffold across which to link pendant pharmacophoric features. Despite the relative lipophilic nature of this small ring, incorporation of the CyBu group often leads to improved PK profiles, through enhanced metabolic stability or solubility.

Oxetanes

Introduction

Oxetanes underwent a renaissance in the late 2000s, sparked by interest in their application as liponeutral *gem*-dimethyl isosteres and replacements for metabolically labile carbonyl functionality. In the following decade, substantial advances towards synthetic approaches[80,81] facilitated application of

oxetanes in drug discovery projects, leading to an improved appreciation of how this small ring may be leveraged to solve medicinal chemistry problems. Whilst 3-substituted oxetanes are predominant in the medicinal chemistry literature, 2- and poly-substituted oxetanes remain relatively underexplored (beyond taxane derivatives).

Over the past decade, there has been a general increase in the number of drug substance patents exemplifying oxetanes (Fig. 2). Currently, 3 taxane derivatives represent the only marketed drugs containing an oxetane, but a further 28 compounds (9 of which are not taxane-related) are in phase I–III clinical trials.[28]

## Structural features and physicochemical properties of oxetanes

The oxetane moiety is small and polar, occupying an equivalent volume to a *gem*-dimethyl group[82] and possessing a dipole comparable to a carbonyl functionality.[83] Oxetanes are relatively flat compared to carbocyclic CyBu rings, as the oxygen atom reduces the number of *gauche* interactions present:[80] the median puckering angle of oxetanes is 7.0° compared to 15.5° for CyBu rings (Fig. 1). The median COC bond angle is 91.3°. Notably, this strained COC bond angle exposes the oxygen lone pairs increasing Lewis basicity, such that oxetanes are excellent hydrogen bond acceptors. Oxetane has the highest hydrogen bonding avidity of the cyclic ethers,[84] and exceeds that of aliphatic aldehydes, esters and ketones (but not amides).[4]

Medicinal chemistry applications of oxetanes

Due to its small size and polar nature, oxetane functionality has gained popularity as a physicochemical property modulating group capable of improving the drug likeness of molecules. In addition, the *gauche*-directing effect of this small ring (*vide infra*) has been used to conformationally bias molecules for improved protein interactions. Finally, oxetanes have been proposed and utilised as property-favourable or chemically stable isosteres of multiple functional groups. The following sections describe contemporary application of oxetanes, and reported limitations.

Reducing lipophilicity. Müller *et al.* demonstrated that replacement of a methylene unit with an oxetanyl moiety at various locations on test substrates consistently led to $\text{Log} P$ reductions ($\sim -0.5 < \Delta \text{Log} P \leq -1.5$).[4] Furthermore, $\text{Log} P$ reduction is even more pronounced when replacing structurally similar lipophilic appendages, such as *gem*-dimethyl, CyPr or CyBu groups.[85] In this regard, oxetanes are useful groups for improving lipophilicity-driven negative endpoints, such as diminished aqueous solubility, metabolic instability, off-target promiscuity, hERG and CYP450 inhibition.

White and co-workers recently demonstrated use of an oxetane moiety to reduce the lipophilicity of a series of indoleamine-2,3-dioxygenase-1 (IDO1) inhibitors, leading to
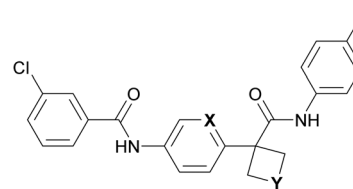
Cmpd	X	Y	LogP[a]	Solubility[b] (µM)	Hep Cl$_{int,u}$ human/rat (mL/min/kg)
36	C	CH$_2$	5.3	2	2000/2000
37	C	O	3.8	76	420/250
38	N	O	3.1	170	<44/<84

Fig. 18 Reducing lipophilicity of IDO1 inhibitors through oxetane incorporation.[86] [a]Log P = Alog P_{98}.[44] [b]Fasted state simulated intestinal fluid (FaSSIF) solubility measured at pH 6.5.

significantly improved PK parameters.[86] CyBu **36** demonstrated high potency, but suffered from limited solubility and extensive metabolism in an *in vitro* hepatocyte assay, both of which were attributed to excessive lipophilicity ($\text{Log} P = 5.3$).[44] Replacement of the CyBu with an oxetane in **37** significantly reduced lipophilicity (1.5 log unit decrease), greatly improving solubility and metabolic stability (Fig. 18) whilst retaining potency. Replacement of the central benzene with a pyridine in **38** led to further physicochemical and ADME improvements, ultimately translating to a low human QD dose prediction of 26 mg for **38**.

Attenuating amine basicity. Oxetanes can have significant impact on proximal amine basicity as a result of strong σ-electron withdrawing character. This effect is greatest when the oxetane is α relative to an amine, but can extend further: Müller and co-workers demonstrated a 0.3 pK_a unit reduction for a δ-aminooxetane relative to the parent alkylamine (Fig. 19).[4] Whilst amine pK_a reductions may be accompanied by significant $\text{Log} D$ increases, in many contexts $\text{Log} D$ may be reduced despite attenuated basicity (*e.g.* replacing a lipophilic group with an oxetane). Lipophilic basic amines are associated with a greater risk of hERG inhibition, phospholipidosis and undesirable PK profiles. Consequently, oxetane installation proximal to an amine represents a strategy to overcome these issues.

Scientists at Vertex Pharmaceuticals identified cyclobutyl amines *e.g.* **39** and **40** as potent protein kinase Cθ (PKCθ) inhibitors (Fig. 20).[87] These compounds however, showed
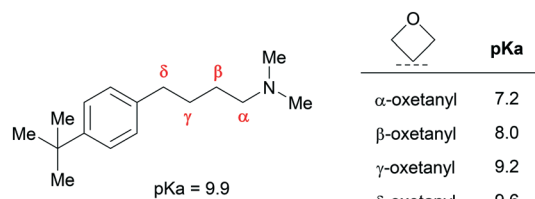

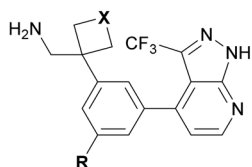|	pKa
α-oxetanyl	7.2
β-oxetanyl	8.0
γ-oxetanyl	9.2
δ-oxetanyl	9.6

Fig. 19 Effect of oxetane introduction on amine pK_a for a series of alkylamines.[4]

Fig. 20 Reducing hERG inhibition of PKCθ inhibitors through oxetane incorporation.[87] [a]Rat liver microsomes. [b]Human liver microsomes. [c]% remaining after 30 minutes incubation. [d]Not determined.

Cmpd	X	R	LogD$_{7.4}$	pK$_a$	hERG IC$_{50}$ (μM)	RLM[a]/HLM[b] stability (%)[c]
39	CH$_2$	H	n.d.[d]	8.8	3	88 / 81
40	CH$_2$	Me	2.9	8.8	0.7	56 / 81
41	O	H	1.7	7.6	>10	77 / 100
42	O	Me	2.2	7.9	>10	59 / 86

Fig. 22 Improving efflux of DLK, MAP3K12 inhibitors *via* oxetane incorporation.[89] [a]MDCK-MDR1 permeability; AB = apical-to-basolateral; BA = basolateral-to-apical. [b]Piperidine pK$_a$ values were calculated using ACDLabs.[90] [c]Topological polar surface area.

Cmpd	R$_1$	R$_2$	Efflux Ratio BA/AB (AB)[a]	Calc pK$_a$[b]	tPSA[c]
47	H	cyPent	95 (0.2)	10.1	78
48	oxetanyl	cyPent	1.4 (8.8)	7.7	78
49	oxetanyl	*i*Pr	1.9 (9.3)	7.7	79
50	acetyl	*i*Pr	9.1 (2.1)	n/a	86

significant hERG inhibition. Judicious replacement of the carbocycle with an oxetane afforded less basic and less lipophilic amines **41–42** with ablated hERG activity and maintained PKCθ inhibition. Furthermore, the oxetanes demonstrated maintained or improved metabolic stability, and improved CYP450 inhibition profiles.
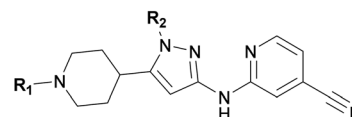
A team at Roche identified a series of respiratory syncytial virus fusion (RSVF) inhibitors reliant on a pendant basic amine for antiviral activity.[88] The lipophilic nature of these basic compounds manifested in high volume of distribution values (V_{ss}; *e.g.* compound **43**, Fig. 21), which concerned the authors due to a perceived risk of accumulation and associated toxicity. To overcome this, oxetane inclusion was investigated. Oxetanes **44–45** retained potent activity relative to **43**, whilst α-aminooxetane **45** demonstrated reduced amine basicity resulting in a lower V_{ss}, comparable to non-basic alcohol **46**.

Amine pK$_a$ can also impact on efflux transporter recognition. During the development of a series of dual

leucine zipper kinase (DLK, MAP3K) inhibitors, Genentech scientists identified piperidine **47** which demonstrated efflux incommensurate with the desired CNS exposure (Fig. 22).[89] Capping the piperidine with an oxetane simultaneously reduced hydrogen bond donor count and amine pK$_a$ whilst maintaining topological polar surface area (tPSA), affording **48** and **49** that demonstrated low efflux. Notably, non-basic acetyl **50** showed an insufficient improvement in efflux ratio, likely due to the higher tPSA.

Conformational preferences of oxetanes. A reported analysis of the Cambridge Structural Database revealed the CH$_2$-R^1 group α to a 3,3-disubstituted oxetane preferentially adopts a torsional angle of $\tau = \pm 120 \pm 30°$ (a *gauche* backbone arrangement) in contrast to a *gem*-dimethyl group which is equally likely to adopt $\tau = 0 \pm 30°$ (an antiperiplanar conformation; Fig. 23).[4] Scientists at Roche working on a series of RSVF inhibitors identified that the potency of *gem*-dimethylamine **51** could be enhanced through oxetane incorporation.[91] Modelling suggested the NH$_2$ interacted favourably with the protein when the alkyl chain adopted a *gauche* conformation, as predicted more likely for oxetane **52**.

Fig. 21 Improving the PK of RSVF inhibitors *via* incorporation of an oxetane.[88] [a]Log D = machine learning Log D. [b]Volume of distribution at steady state.

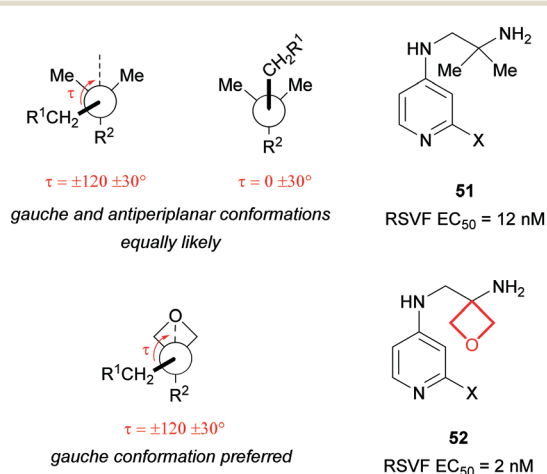| Cmpd	LogD[a]	NH$_2$ pK$_b$	V_{ss}[b] (iv, L/Kg)
43	0.9	10.4	17
44	1.1	9.9	20
45	2.2	8.0	4.1
46	2.6	n/a	2.5

Fig. 23 Comparison of conformational preferences of alkyl chains bearing an oxetane *vs.* a *gem*-dimethyl group and effect on potency for a matched pair of RSVF inhibitors (X = undisclosed substitution).[91]

Oxetanes as isosteres. Within drug molecules, carbonyl functional groups can be susceptible to chemical and metabolic instability, and α-stereocenters may be liable to racemisation. Oxetane has a comparable dipole, and similar lone pair spatial orientation and hydrogen bonding capabilities to the C=O group. Consequently, oxetane derivatives have been proposed as stable isosteres of ketones,[4] esters,[92] thioesters,[93] carboxylic acids,[94] amides,[92] cyclic ketoamines and lactams,[4] and glutarimides[95] (Fig. 24). However, it should be noted that oxetane isosteres differ from their carbonyl counterparts in lateral bulk, non-bonded C O distance, conformational preference and mesomerism. For example, non-hydrolysable oxetanyl peptidomimetics possess the same hydrogen bond donor and acceptor pattern to a peptide,[5] but introduce a basic amine and likely assume different low energy conformations to the parent peptide.[96]

Oxetanes have also been proposed as property-enhancing isosteres of the *gem*-dimethyl group, *t*-butyl group,[54,97] CyPr, CyBu,[85] and morpholine.[82] Of particular note, homospiromorpholine **53** represents a highly soluble fragment, capable of greatly increasing aqueous solubility above and beyond the morpholine matched pair.[4]

Liabilities associated with oxetanes

Metabolism of oxetane substructures. Whilst oxetane incorporation can positively impact physicochemical properties and ADME parameters, the oxetane units themselves may be liable to metabolic biotransformation, depending on overall chemical context of the molecule. For example, Rioux and co-workers showed the major metabolites of the first-in-class protein arginine methyltransferase-5 (PRMT5) inhibitor EPZ015666 (**54**) were hydroxypropionic acid **55** and diol **56**, formed *via* CYP450-mediated oxidative scission of the oxetane followed by oxidation or reduction of the intermediate aldehyde (Fig. 25).[187]
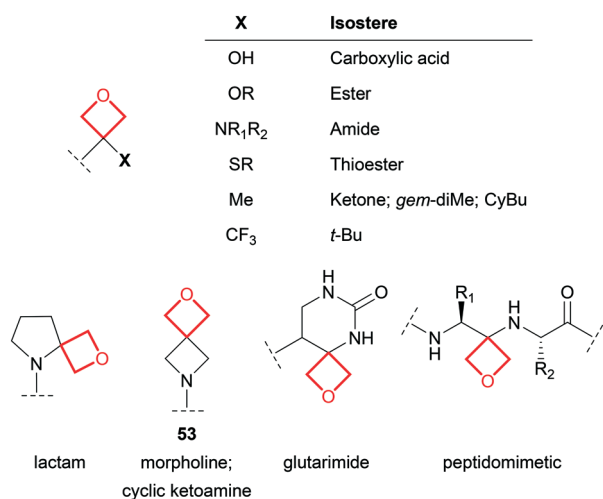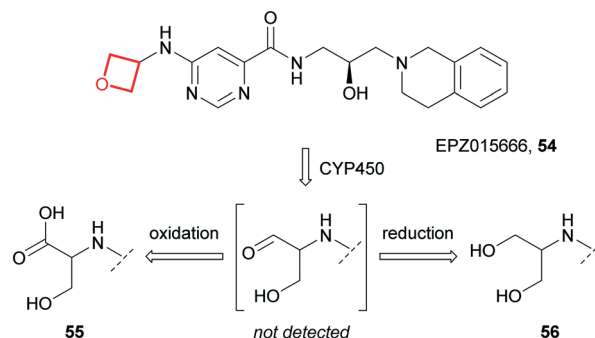

Fig. 25 The major metabolites of EPZ015666 (**54**), formed *via* CYP450-mediated oxidation of the oxetane ring.[187]

In addition to turnover *via* redox pathways, oxetane-containing molecules may be substrates of liver microsomal epoxide hydrolase (mEH),[98,99] forming a diol metabolite *via* hydrolysis (akin to **56**). Toselli *et al.* demonstrated that spirocyclic, bridged bicyclic and straight chain oxetanes can be turned over by mEH.[100] The authors noted no correlation between extent of hydrolysis by mEH and physicochemical properties (Log D, pK_a, LUMO energy), whilst minor structural changes had significant impact (Fig. 26), implicating global structural recognition as a key factor for susceptibility to mEH turnover. It was suggested that oxetanes may provide handles to reduce dependency on CYP450-mediated clearance to minimise risk of drug–drug interactions, although PK predictions would likely present a challenge.

Hydrolytic instability of oxetanes. Although substantially less reactive than the smaller homologue epoxide, the ring strain (25.3 kcal mol^{-1})[80] and Lewis basicity associated with oxetanes render this small ring prone to acid-catalysed ring opening. Indeed, this makes oxetanes useful synthetic intermediates.[80] This instability to protic conditions however, can be problematic in the context of medicinal chemistry applications. For example, in one study a range of 3-monosubstituted oxetanes showed limited stability in acidic aqueous media.[4] However, it should be noted that this liability is entirely context specific and should be assessed for different oxetanes; in the same study, 3,3-disubstituted oxetanes were found to be much more stable, fully recoverable after 2 hours from buffered aqueous solutions over the pH range 1–10 at 37 °C.

Outlook

The oxetane ring has become an established part of the medicinal chemistry toolbox, with applications focussing on

X	Isostere
OH	Carboxylic acid
OR	Ester
NR$_1$R$_2$	Amide
SR	Thioester
Me	Ketone; *gem*-diMe; CyBu
CF$_3$	*t*-Bu

lactam   morpholine; cyclic ketoamine   glutarimide   peptidomimetic

53

Fig. 24 Examples of proposed oxetanyl isosteres of various functional groups.
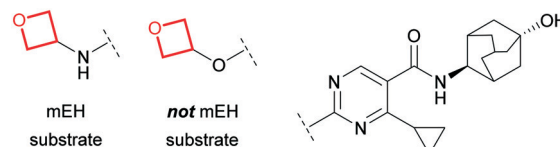

mEH substrate   *not* mEH substrate

Fig. 26 Subtle structural changes can influence mEH recognition.[100]

property enhancement owing to its small and polar nature. Whilst reported applications predominantly utilise 3-substituted oxetanes, judicious incorporation of 2- and poly-substituted oxetanes remains underexplored. This imbalance may shift as novel, simplified synthetic approaches to more elaborate oxetane motifs are developed.

Azetidines

Introduction

Azetidines are polar, rigid 4-membered rings distinct to their neutral small ring congeners because of their basic nitrogen atom.[101,102] Despite the prevalence of the larger cyclic amine homologues pyrrolidine and piperidine,[103] azetidines feature in only 9 approved drugs[28] which is undoubtedly due in part to their challenging synthesis.[104] Nevertheless, an increasing number of synthetic methods to form and append azetidines to molecules[104–106] has given them significant prominence in drug discovery in recent years (Fig. 2).
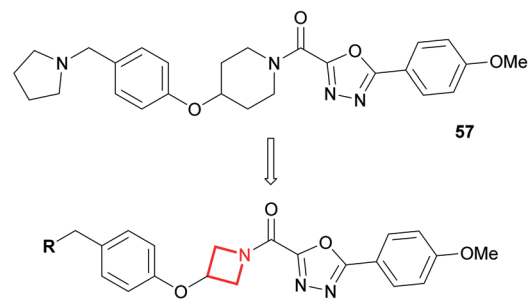
Structural features and physicochemical properties of azetidines

Azetidines share similar median bond lengths and angles to CyBu rings, with the exception of the CNC bond angle when the nitrogen is sp^2 hybridised (Fig. 1). The median puckering angle of azetidines with sp^3 hybridised nitrogens (15.3°) is similar to that of CyBu (15.5°) and expectedly, significantly larger than for the flatter sp^2 analogues (6.4°). Furthermore, the calculated ring strain of azetidine is much larger than that of piperidine (25.2 $vs.$ 0 kcal mol^{-1} respectively)[107,108] and pyramidal inversion of the nitrogen is facile at room temperature ($\Delta G^{\neq}$ = 10 kcal mol^{-1} for N-methyl azetidine in the liquid phase).[109] Finally, in aqueous solution at 25 °C, the pK_a of azetidine (11.29) is similar to pyrrolidine (11.27) and piperidine (11.22), yet distinct to that of aziridine (8.04).[23]

Medicinal chemistry applications of azetidines

The small size, polarity, high Fsp^3 character, basicity and rigidity of azetidines can often improve the global properties of molecules, $e.g.$ lipophilicity, solubility, $in vitro$ metabolism and PK. Notably, azetidines have found particular prominence as replacements for numerous functionalities including pyrazine,[110] piperidine,[111–113] pyrrolidine,[114] diazepane,[115] β-lactam,[116] pyrrolidinone,[117] piperazine,[118] CyPr,[119] and proline.[120] In this section, recent noteworthy applications of azetidines have been captured, as well as examples of reported liabilities.

Reducing lipophilicity. The symmetric nature of 1,3-substituted azetidines make them viable replacements for 1,4-substituted piperidines. A team at AstraZeneca recently reported the discovery of a melanin concentrating hormone receptor 1 (MCHr1) antagonist **57** with markedly lower lipophilicity compared to previously reported antagonists (Fig. 27).[111] Aiming to further reduce lipophilicity whilst
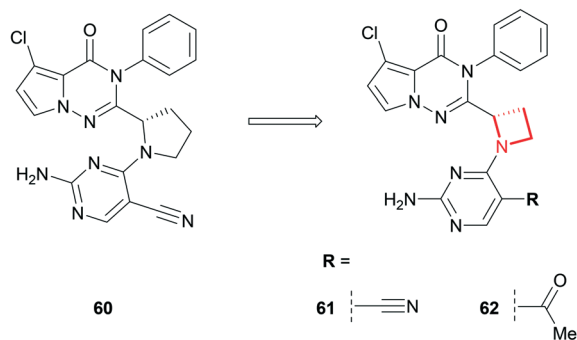

Fig. 27 Discovery of azetidine-containing MCHr1 antagonist AZD1979 (**59**).[111] ^{a}Functional [^{35}S]GTPγS assay developed for MCHr1. ^{b}Caco-2 permeability; AB = apical-to-basolateral; ER = efflux ratio.

Cmpd	R	MCHr1 IC$_{50}$ (nM)^a	LogD$_{7.4}$ (LLE)	hERG IC$_{50}$ (μM)	Caco-2 AB (ER)^b
57	n/a	28	2.3 (5.3)	11.0	46 (0.23)
58		34	1.8 (5.7)	5.5	35 (0.37)
59		27	2.0 (5.6)	22.0	61 (0.46)

maintaining the favourable CNS properties of **57**, the team proposed an azetidine replacement for the piperidine core (**58**). It was postulated that this could project the key pharmacophoric features in similar positions to the putative bioactive conformation of piperidine-containing agonists such as **57**. Indeed, this transformation resulted in an overall increase in LLE, with Caco-2 permeability and efflux only marginally affected (**57** $vs.$ **58**). Despite the reduction in Log D, hERG inhibition remained a concern. Nevertheless, this reduction enabled the broader scoping of SAR on the periphery of **58**. This culminated in the discovery of AZD1979 (**59**), where in fact the azetidine-containing 2-oxa-6-azaspiro[3.3]heptane replacement of the pyrrolidine provided the desired wider selectivity margin over hERG inhibition. This change led to a decrease in pK_a (from 9.9 to 8.2 for **58** and **59** respectively) which likely contributed to the reduced hERG activity, despite a slight increase in Log D.[111]

A similar ring contraction strategy was reported by scientists at Janssen and Hutchinson MediPharma, who demonstrated that the 1,2-substituted pyrrolidine core of a series of selective PI3Kγ/δ dual inhibitors ($e.g.$ **60**) could be replaced with a 1,2-disubstituted azetidine ($e.g.$ **61**), leading to reduced lipophilicity and improved microsomal stability (Fig. 28).[114] Modification of the pyrimidine substitution of **61** afforded the highly potent and kinome-selective **62**, a promising pre-clinical candidate that demonstrated desirable PK properties and good efficacy in an $in vivo$ arthritis model.

Solubility enhancement. Azetidines have also been used to replace unsaturated ring systems.[110] Towards the discovery of potent and selective phosphodiesterase 10A (PDE10A)

Fig. 28 Replacement of the 1,2-disubstituted pyrrolidine core of a series of PI3Kγ/δ dual inhibitors with an azetidine.[114] [a]Log D = AZ log D, calculated Log D at pH 7.4. [b]Rat liver microsomes. [c]Human liver microsomes. [d]% remaining after 30 minutes incubation. [e]Not determined.

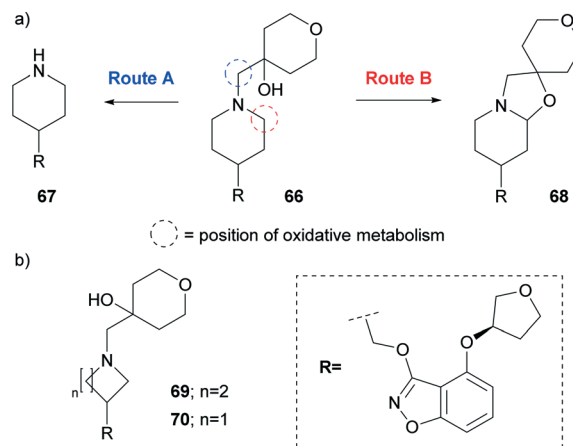| Cmpd	PI3Kγ IC$_{50}$ (nM)	PI3Kδ IC$_{50}$ (nM)	LogD$_{7.4}$[a]	RLM[b]/HLM[c] stability (%)[d]
60	7	1	2.8	24 / n.d.[e]
61	27	12	2.4	78 / 71
62	4	5	2.4	64 / 82

Fig. 29 Solubility enhancements in Amgen's PDE10A inhibitor drug discovery program.[121,123] [a]Log D = AZ log D, calculated Log D at pH 7.4. [b]Aqueous solubility measured at pH 7.4 using a phosphate buffered saline solubility assay.
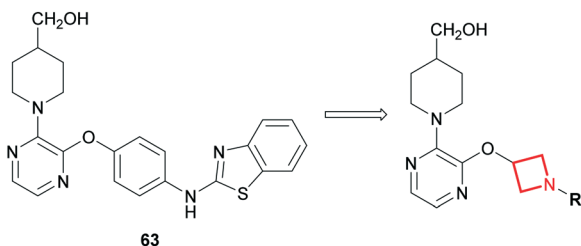
Cmpd	R	PDE10A IC$_{50}$ (nM)	LogD[a]	Solubility[b] (μM)
63	n/a	0.2	3.88	6
64		21	2.84	31
65		2.4	2.94	178

inhibitors for the treatment of schizophrenia,[121] scientists at Amgen noted that the low aqueous solubility of inhibitor 63 (ref. 122) could prove challenging to its further development (Fig. 29). This was attributed to a high degree of aromaticity, known to limit aqueous solubility.[1,9,10] As a result, saturated heterocycles were proposed as replacements to the central aromatic ring. Molecular modelling assisted in concluding that an azetidine replacement may be tolerated. Despite a 100-fold loss in potency for azetidine 64, the authors were satisfied with the 5-fold improvement in solubility. Further optimisation culminated in a novel series of soluble and potent PDE10A inhibitors (*e.g.* 65) demonstrating >1000-fold

selectivity over other PDEs.[121,123] In parallel to increasing the Fsp[3] character of the inhibitors, the azetidine ring contributes to a predicted reduction in Log D, which would be conducive to increasing solubility.

Shifting metabolism. Scientists at Pfizer recently disclosed a partial agonist of the human 5-hydroxytryptamine receptor 4 (5-HT$_4$), PF-04995274 (66).[113] After dosing volunteers with 66, metabolites 67 and 68 were detected in pooled plasma (Fig. 30a). In fact, 68 was found in higher abundance than the parent drug, despite only being a minor component in *in vitro* experiments.[113,124] Compound 67 is believed to be formed *via* an oxidative dealkylation (route A), whereas 68 is generated *via* the intramolecular trapping of an oxidatively formed iminium species (route B).[125] Concerns around the off-target pharmacology of the metabolites led to the exploration of replacements of the piperidine. A pyrrolidine variant 69 generated the two analogous metabolites whereas azetidine 70 showed neither (Fig. 30b). Interestingly, for the latter, a metabolic shift was observed where hydroxylation of the benzisoxazole ring became the predominant metabolic route. This shift was attributed to the higher calculated energy barrier for abstraction of the hydrogen on the α-carbons to the azetidine nitrogen compared to that of the larger azacycles. The replacement also resulted in a drop in Log D, reduced intrinsic CYP450-mediated turnover and thus a lowering of the predicted human intrinsic clearance, all whilst retaining functional potency.

Reducing metabolism. Like CyBu rings, azetidines have also been used to constrain linkers, particularly in the field of sphingosine-1-phosphate receptor 1 agonists, as

Fig. 30 a) Metabolites observed in pooled human plasma for PF-04995274 (66). b) Optimisation of the 5-HT$_4$ partial agonist.[125] [a]cAMP HTRF agonist assay. [b]Human liver microsomes scaled to the whole liver using physiological parameters (not corrected for incubational binding).

Cmpd	5HT$_4$ EC$_{50}$[a] (nM)	LogD$_{7.4}$	Scaled Clint[b] (mL/min/Kg)
66	0.4	1.2	33
69	3.5	0.8	48
70	7	0.6	21

β-alanine[126] and γ-aminobutyric acid[127,128] replacements. In a related case-study, scientists at Aurigene replaced a linear tertiary amide in the enoyl-[acyl carrier protein] reductase (FabI) inhibitor AFN-1252 (ref. 129) (**71**) with an azetidine amide (**72**) (Fig. 31).[130] Despite the introduction of an extra carbon, a significant improvement in stability towards mouse liver microsomes was observed, translating to an improved mouse PK profile.[131] This was credited to the cyclic and conformationally restricted azetidine amide which was claimed to be more resistant to enzymatic hydrolysis than the linear analogue. The azetidine in **72** likely also benefits from a relatively higher energy barrier for oxidative N-dealkylation,[113] although this was not discussed in the report. Comparable activity for FabI was reported, coupled with good cellular activity and *in vivo* efficacy in a murine systemic infection model.

Linkers in the beyond-rule-of-5 (BRo5) chemical space. Alongside azetidines, the more elaborate azetidine-containing spirocycles (Fig. 32) have tremendous capacity in modulating the overall properties of molecules.[132–134] This, combined with their rigidity, aptness for exploration of 3D space[80] and also their versatility as reagents, makes these azetidine substructures ideal for implementing in proteolysis targeting chimera (PROTAC) drug discovery programs.[135,136] PROTACs tend to occupy the BRo5 chemical space where oral absorption constitutes a significant challenge. The linker in these bifunctional molecules has been recognised as one of the key design features as it: a) needs to connect and project the target protein and E3 ligase ligands in a fashion conducive for degradation and b) can significantly modulate the global physicochemical properties. In the advent of this modality, it is interesting to see that amongst others,

azetidines and spiro-azetidines appear to play an important part in the sampling of chemical space as can be seen from examples taken from recent publications[137,138] and patent filings (*e.g.* **73**;[137] **74**;[139] **75**;[140] Fig. 32).
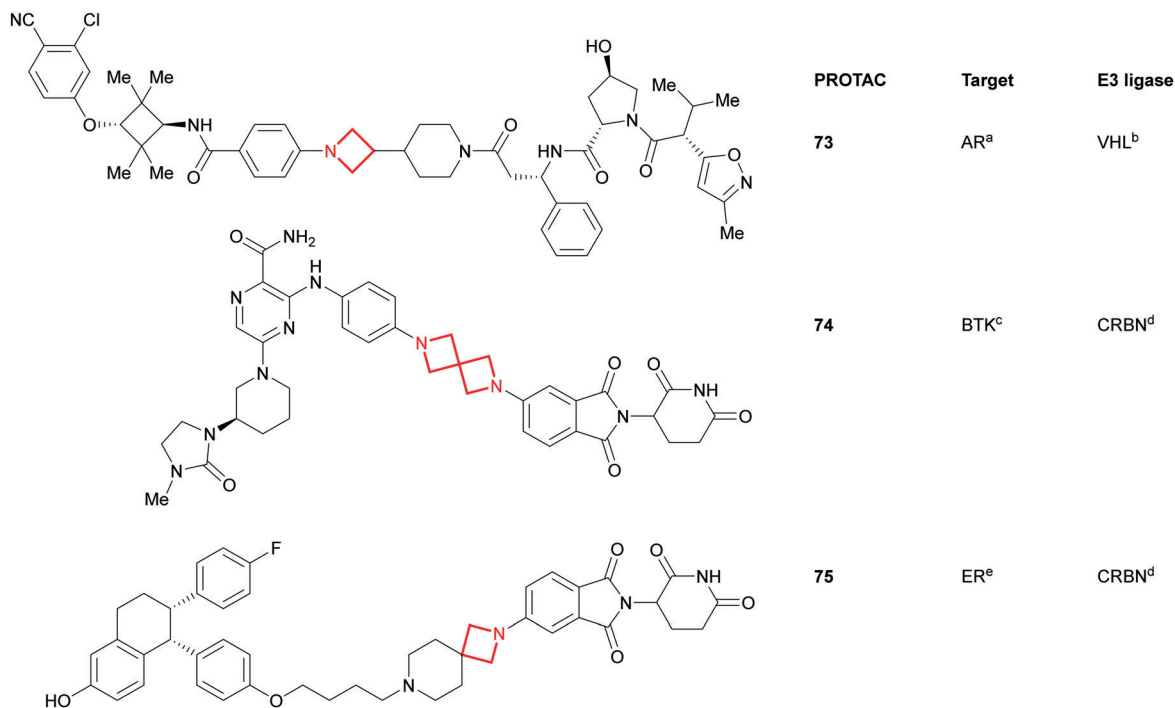
Similarly, azetidines have also been used as tethers to ketolides in the search for novel broad spectrum antibiotics. One of the key features of telithromycin (**76**), responsible for its efficacy in erythromycin resistant strains, is the alkyl–aryl tether of the ketolide scaffold (Fig. 33).[141] Aiming to develop an antibiotic which matches the efficacy of **76**, yet is devoid of its reported hepatotoxicity,[142] scientists at Pfizer replaced the alkyl tether with an azetidine functionality.[143] This rigid ring constrains the tether and modulates the global properties of the molecule by introducing polarity and basicity. The nucleophilic handle off the ketolide also facilitated the broad exploration of SAR of the pendant group resulting in the clinical candidate **77** which has an improved metabolic and safety profile compared to **76**.

Liabilities associated with azetidines

Chemical stability. Similar to aziridines, azetidines can undergo ring opening reactions,[104,105] albeit at a much slower rate.[144] During the scale-up of the glucokinase activator AZD1656 (**78**), scientists at AstraZeneca noted that **79** was formed alongside **78** on the final amide coupling step (Fig. 34).[145] It was concluded that the HCl by-product of the reaction led to the activation and subsequent ring opening of the azetidine in **78**. A mitigation strategy employed a pyridine scavenger in the reaction, which was removed using sulfuric acid instead of HCl during aqueous work-up, to avoid the formation of **79**. Similar intermolecular ring openings have been reported for azetidine hydrochloride salts which can dimerise upon standing.[146,147]

A related ring opening was observed by scientists at Pfizer who noted a significant chemical instability of their PDE9A inhibitor **80** in acidic and neutral media (Fig. 35a).[148] After performing analytical investigations on a model system (**81**) in aqueous HCl, the team concluded that the pendant pyrimidine participates in an intramolecular ring opening of the azetidine, resulting in the formation of **82** following the addition of water (Fig. 35b). Optimisation of the series focussed on distorting the trajectory of the pyrimidine intramolecular attack. Lead compound **83**, which lacks the oxygen linker to the pyrimidine, showed improved stability with no decomposition observed after 10 hours at pH <2.

GSH reactivity. Metabolite identification studies of the aforementioned AZD1979 (**59**) in human hepatocytes revealed an unusual glutathione (GSH) ring opening of the spiro-azetidine (Fig. 36).[149] This is a glutathione transferase-catalysed transformation and does not occur in the absence of this enzyme, nor is it a result of any prior bioactivation catalysed by CYP450s. Fortunately, the GSH-conjugated metabolite (**84**) was not a toxicological concern towards the advancement of AZD1979 into clinical development.

Fig. 31 Conformational restriction of FabI inhibitors and their effect on *in vitro* metabolism and *in vivo* PK.[130] [a]*In vitro* metabolism study in mouse liver microsomes; value indicates % of compound remaining after a 60 min incubation. [b]Single dose in mice (P.O., 10 mg kg⁻¹). [c]Area under plasma concentration time curve.

| Cmpd	FabI IC₅₀ (nM)	MLM stability[a] (%)	Pharmacokinetics[b]		
			AUC[c] (μg/mL*h)	Cmax (μg/mL)	t₁/₂ (h)
71	29	17.5	2.20	0.44	1.84
72	141	55.7	63.5	8.95	3.20

Fig. 32 Azetidine- and spiroazetidine-containing PROTACs. PROTACs are aligned with the target binding ligand, linker and E3 ligase binding ligand from left to right. [a]Androgen receptor; [b]Von-Hippel Lindau; [c]Bruton's tyrosine kinase; [d]cereblon; [e] estrogen receptor.

PROTAC	Target	E3 ligase
73	AR[a]	VHL[b]
74	BTK[c]	CRBN[d]
75	ER[e]	CRBN[d]

N-Acryloyl azetidines have been explored in programs where covalent inhibition of a target is the desired mechanism of action.[150,151] In such programs, the reactivity of the electrophile needs to be fine-tuned to enable potent and selective inhibition of the target, whilst evading any significant GSH-induced metabolism.[152,153] Remarking on the rarity of *N*-acryloyl azetidines in drug discovery, scientists at Eli Lilly assessed the susceptibility of these electrophiles to GSH conjugation in phosphate buffer. A significantly higher reactivity compared to their open chain analogues was reported (*e.g.* **85** *vs.*. **86**, Fig. 37a).[154] This was attributed to the reduced amide character of *N*-acylazetidines, caused by non-planarity, and thus a higher electrophilicity of the conjugated double-bond.[154,155] A team at Novartis recently reported the low plasma stability of the Bruton's tyrosine kinase (BTK) inhibitor **87** which was credited to the aforementioned reactivity.[156] This was deprioritised in favour of the open-chain variant which is found in remibrutinib (**88**; Fig. 37b).

Outlook

Azetidines represent the smallest stable azacycle used in medicinal chemistry. Like many functional groups, azetidines can carry certain liabilities worth interrogating. However, their unique characteristics can impart significant benefits to the global properties of molecules. This, coupled with the ease of functionalisation on the nitrogen atom, make them particularly valuable scaffolds in drug discovery programs.
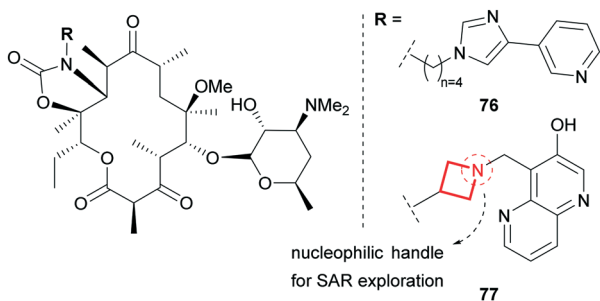
Fig. 33 Azetidine as a tether in the optimisation of ketolide antibiotics.[143]
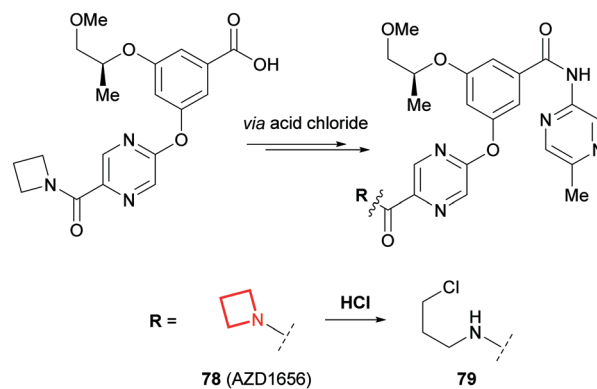
Fig. 34 Hydrochloric acid promoted ring opening of the azetidine in AZD1656 (**78**).[145]

a)

b)

Fig. 35 a) Overall modification of the PDE9A inhibitor **80**. b) Intramolecular ring opening of the azetidine-containing model system (**81**).[148]

R =

Fig. 36 Glutathione transferase catalysed metabolism of AZD1979 (**59**).[149]

Bicyclo[1.1.1]pentanes

Introduction

The bicyclo[1.1.1]pentane (BCP) motif is the smallest of the bridged aliphatic ring systems and has gained prevalence within medicinal chemistry predominantly for its application as a saturated benzene isostere. Despite the first instance of its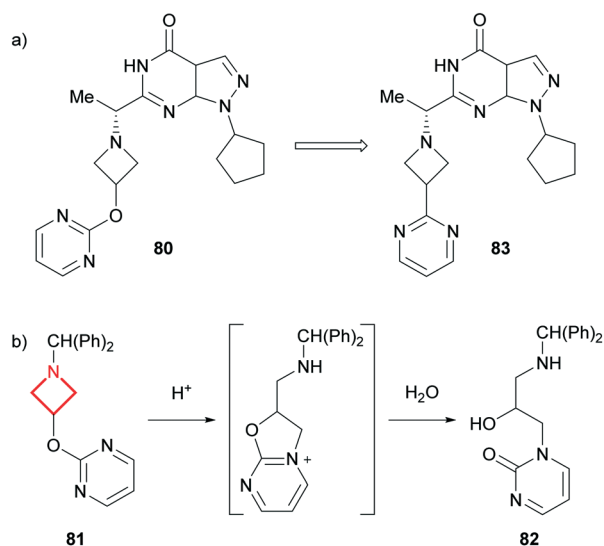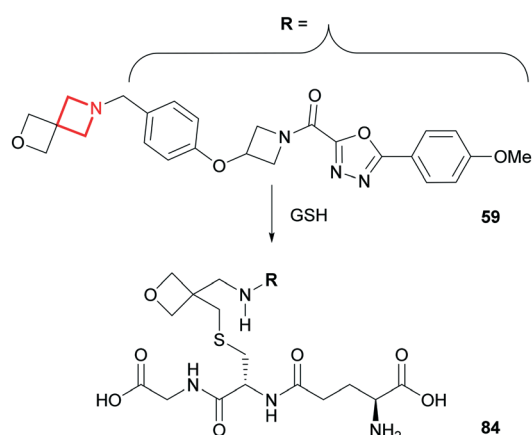 successful bioisosterism in 1996,[157] the BCP moiety has yet to appear in any approved drug scaffolds, although it has appeared in an increasing number of patents over the past decade (Fig. 2), likely in part due to recent advances in efficient BCP synthesis.[158–166] The use of the BCP motif as an alkyne isostere[167] or a *t*-Bu isostere[3,168] has been less thoroughly explored.

Structural features and physicochemical properties of bicyclo[1.1.1]pentanes

The BCP ring system has largely been employed to improve physicochemical and PK properties relative to phenyl
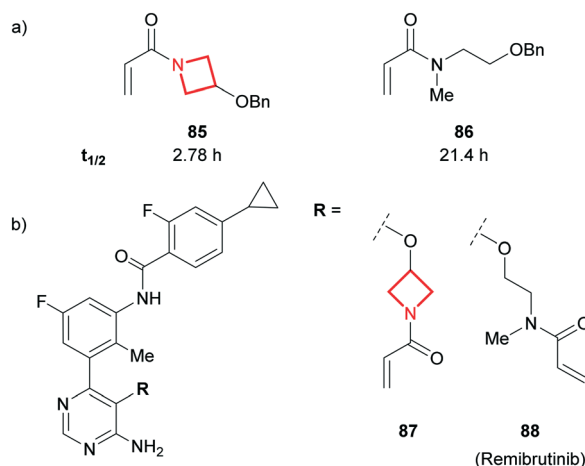
a)

b)

Fig. 37 a) Half-life ($t_{1/2}$) measurement at 0.1–1 mM of acrylamide, 10 mM glutathione, 70 mM phosphate buffer (pH = 7.4), 30% MeCN at 37 °C.[154] b) Novartis' acrylamide BTK covalent inhibitors.[156]

analogues. BCPs have a median non-bonded C C distance of 1.87 Å and an approximately linear substitution vector arrangement: the median carbon bridgehead substituent angle is 178.4° (Fig. 1). While the BCP ring positions opposite substituents in a near-linear fashion, mimicking that of a *para*-substituted benzene, the BCP presents a shorter non-bonded C C distance relative to its phenyl counterpart (2.79 Å for benzene).[169] As a result of its rigid 3D character, replacement of phenyl with a bridged BCP ring increases Fsp^3 consequently disrupting planarity, limiting intermolecular π-stacking and likely imparting improvements in solubility. Generally, a reduction in lipophilicity can also be observed for BCP-analogues relative to phenyl rings. Benefits of reduced lipophilicity include a reduced likelihood of non-specific binding and generally lower metabolic clearance of resulting compounds.

Medicinal chemistry applications of bicyclo[1.1.1]pentanes

Due to its rigid 3D character and linear positioning of its substituents, the BCP ring system is becoming a more prominent motif capable of modulating physicochemical properties in pharmaceutical compounds, resulting in an increasing occurrence in medicinal chemistry design strategies.

Phenyl bioisostere. An early example of the application of BCP as a phenyl isostere was demonstrated by Stepan and colleagues from Pfizer, in which a fluorophenyl group in the known γ-secretase inhibitor **89** was replaced with a BCP ring in **90** (Fig. 38).[170]

A significant increase in solubility was observed, attributed to the increased Fsp^3 character, as well as a substantial reduction in lipophilicity. Compound **90** also remained equipotent to **89**, affording a higher LLE, and confirming that the shorter interbridgehead distance of the BCP was well tolerated within the binding pocket. Improved metabolic stability was observed, likely as a result of the
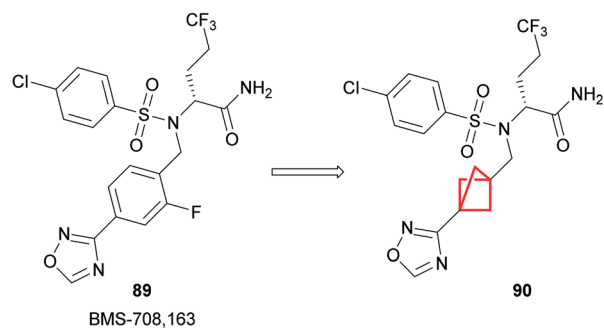
Cmpd	Cell IC$_{50}$ (pM)	LogD$_{7.4}$ (LLE)	HLM^a Cl$_{int,app}$ (mL/min/ kg)	Solubility^b (μM)	RRCK P$_{app}^c$ (10^{-6} cm/s)
89	225	4.70 (5.0)	<16.2	1.70	5.52
90	178	3.8 (6.0)	<8.17	19.7	19.3

Fig. 38 Optimisation of a γ-secretase inhibitor.[170] ^{a}Human liver microsomes; Cl$_{int,app}$ = total apparent intrinsic clearance from scaling *in vitro* $t_{1/2}$ in HLM. ^{b}Thermodynamic solubility measured at pH 6.5. ^{c}Apparent permeability coefficient in Ralph Russ canine kidney (RRCK) cells with low transporter activity.

reduction in Log$D$, as well as improved intrinsic permeability. Compound 90 was also outside of the scope of the patent of the original γ-secretase inhibitor 89.[171]

Similar improvements in metabolic stability, lipophilicity and solubility have been observed through analogous phenyl replacements with BCP.[171–174] For example, recent work from scientists at Merck has shown the use of BCP as a phenyl isostere to address concerns of metabolic instability (Fig. 39). Compound 91 was identified from an automated ligand identification system to have excellent potency against IDO1.[86,175] Compound 91, whilst achieving excellent potency in cell-based and whole cell assays, was limited by poor metabolic stability in both *in vitro* and *in vivo* rat PK studies.

MetID studies identified amide bond cleavage as the predominant metabolic pathway (Fig. 39), generating a potentially mutagenic aniline metabolite.[176] Alternative modifications, including the use of amide bioisosteres, provided insufficient improvement in metabolic stability or led to significant loss of cellular potency. Molecular modelling (later corroborated by X-ray crystallography; Fig. 39 bottom) indicated that the BCP ring could be well tolerated in the binding site, acting predominantly as a linker, presenting an opportunity to mitigate hydrolysis of the amide in compound 91. Direct isosteric replacement of the phenyl group with a BCP in 92 engendered a significant reduction in lipophilicity, albeit with a slight reduction in potency. Subsequent replacement of the α-CyBu with a chiral methyl group (93) could further decrease the lipophilicity and improved both potency and stability, translating to a
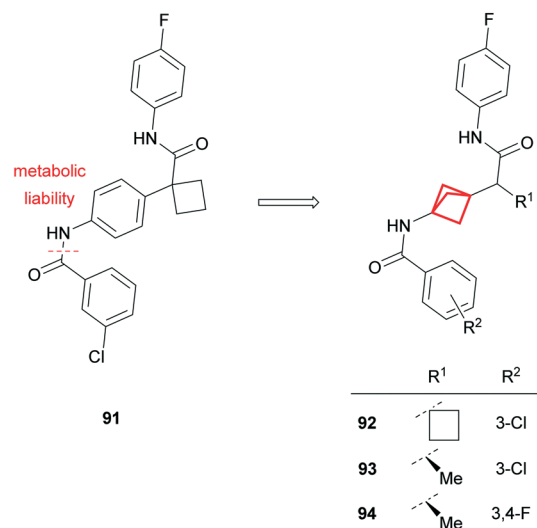
Cmpd	HeLa/hWB^a IC$_{50}$ (nM)	LogP^b	RH^c Cl$_{int}$ (mL/min/Kg)	Cl$_u^d$ (mL/min/Kg)
91	1.7/30	5.3	1935	4371
92	5.2/n.d.^{e}	4.1	n.d.^{e}	n.d.^{e}
93	3.1/121	3.6	248	194
94	1.9/36	3.3	195	37
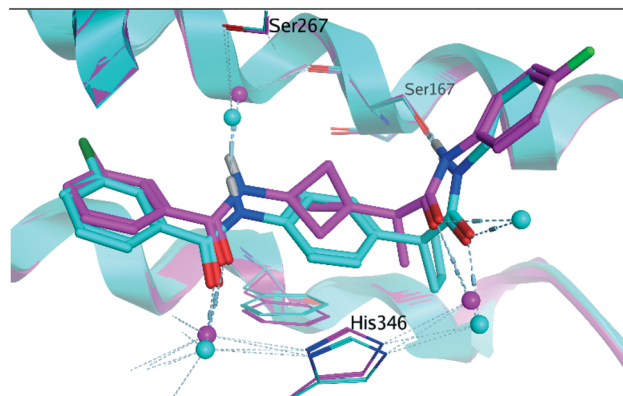
Fig. 39 Top: Development of IDO1 inhibitors.[86,175] ^{a}Human whole blood assay. ^{b}Log$P$ = AlogP_{98}.[44] ^{c}Rat hepatocytes, *in vitro* unbound clearance. ^{d}*In vivo* PK study performed in rat. ^{e}Not determined. Bottom: Overlay of IDO1-bound structures of 93 (magenta; PDB code: 6WJY) and related aryl-linked bisamide (cyan; PDB code: 6V52) illustrating the utility of BCP as an isostere of a phenyl spacer. Water molecules are shown as spheres; hydrogen bonds are shown as pale blue dashed lines.

good overall PK profile including low clearance and excellent oral bioavailability. Further modification of the aryl substituents (R^2) led to the discovery of compound 94, which exhibited excellent potency, good PK and a much lower predicted human dose relative to previously reported IDO1 inhibitors.[86,175]

Aniline bioisostere. Amino-BCPs have also been shown to provide a metabolically stable bioisostere for anilines,
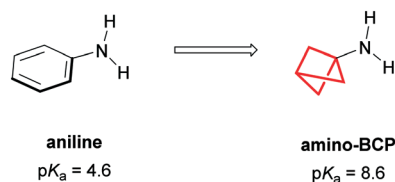
Fig. 40 Amino-BCP as an isostere of aniline.
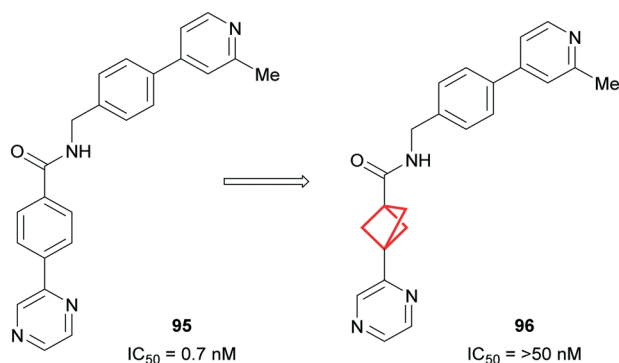
Fig. 41 Replacement of phenyl ring with BCP in known Wnt inhibitor causing loss of biological activity.[183]

proving more resistant to reactive metabolite formation and CYP450 inhibition.[177] However, replacement of an aniline with an amino-BCP can strongly influence the basicity of the nitrogen (pK_a(aniline) = 4.6, pK_a(amino-BCP) = 8.6),[178] changing the ion class of the compound (Fig. 40).[101,102,179]

Limitations of bicyclo[1.1.1]pentanes

Loss of biological activity. While it is evident that physicochemical properties and PK can be improved by replacing a phenyl ring with a BCP motif, this successful isosterism cannot always be achieved. In the event that the phenyl group is important for binding affinity, i.e. through the formation of π-stacking interactions, replacement with a BCP ring can result in significant loss of potency.[180,181] This was exemplified by Adsool and co-workers who found that replacement of the phenyl ring in Wingless Int-1 (Wnt)[182] inhibitor **95** resulted in complete loss of activity for **96** in the cell-based reporter assay (Fig. 41).[183]

Synthetic tractability. Synthetic incorporation of the BCP motif in many cases still remains a challenge and, until recently, efficient synthetic methodologies have been elusive. As a result, commercially available reagents can be limited, expensive and have long lead times. Additionally, due to the difficulty of synthesis of more highly substituted BCP variants, the isosteric replacement of aromatic rings with BCP has largely been limited to mono- or para-substituted benzenes. Isosteric replacement of meta- and/or ortho-substituted benzenes with aliphatic rings remains relatively underexplored.[160,184,185] However, during the preparation of this manuscript, a report describing the synthesis of 1,2-disubstituted BCPs was published, now

facilitating the potential to investigate this substitution pattern for bioisosterism of ortho- or meta-substituted arenes.[186]

Outlook

The use of the BCP ring in medicinal chemistry has largely been precluded by the lack of synthetically tractable access to these novel bioisosteric scaffolds. In recent years the increase in prevalence of the BCP motif has gone hand in hand with the advent of increasingly efficient synthetic methods allowing more facile incorporation of this bicyclic scaffold.[158–166] This is exemplified by the surge of appearances of BCPs in patents in recent years (Fig. 2). With growing attention from the synthetic community regarding access to these scaffolds, and the potential impact on physicochemical properties and PK profiles, the BCP bicyclic ring system will likely become more commonplace within medicinal chemistry.

Conclusions

This review aims to provide a brief comparative overview of the applications of three- and four-membered aliphatic rings to medicinal chemistry drug discovery projects. The small nature of these ring systems often engenders improvements in the physicochemical properties of molecules when replacing larger groups, positively impacting ADME end points such as metabolism and solubility. In addition, the rigid structures of the small rings provides opportunity to design conformationally restricted analogues, enhancing target protein binding affinity through minimised entropic penalties, as well as providing specific vectors between pharmacophoric features. Furthermore, the unique physicochemical, structural and electronic properties of each ring system has been utilised to overcome many other specific medicinal chemistry problems.

Reported medicinal chemistry liabilities are also known for each ring system, illustrated herein to increase awareness. However, it should be noted that many of these shortcomings are likely context specific and may not present when the overall molecular structure differs. A considerable limitation for several of these ring systems is synthetic tractability. Whilst general methods of assembly are reported, protocols for making specific point changes (that would be highly enabling for design of drug molecules) remain limited.

The interest in these small rings will undoubtedly increase as more creative medicinal chemistry applications are demonstrated, and as synthetic methodologies are developed that facilitate access to a more diverse array of substitution patterns. It is anticipated that the existing and newly emerging variants of these systems will continue to feature in future drug discovery programs.

Conflicts of interest

All authors are employees of AstraZeneca.

Notes and references

1 F. Lovering, *MedChemComm*, 2013, **4**, 515–519.

2 H. Sun, G. Tawa and A. Wallqvist, *Drug Discovery Today*, 2012, **17**, 310–324.

3 M. V. Westphal, B. T. Wolfstädter, J.-M. Plancher, J. Gatfield and E. M. Carreira, *ChemMedChem*, 2015, **10**, 461–469.

4 G. Wuitschik, E. M. Carreira, B. Wagner, H. Fischer, I. Parrilla, F. Schuler, M. Rogers-Evans and K. Müller, *J. Med. Chem.*, 2010, **53**, 3227–3246.

5 M. McLaughlin, R. Yazaki, T. C. Fessard and E. M. Carreira, *Org. Lett.*, 2014, **16**, 4070–4073.

6 N. A. Meanwell, *J. Med. Chem.*, 2011, **54**, 2529–2591.

7 N. A. Meanwell, *Chem. Res. Toxicol.*, 2016, **29**, 564–616.

8 C. Jamieson, E. M. Moir, Z. Rankovic and G. Wishart, *J. Med. Chem.*, 2006, **49**, 5029–5046.

9 F. Lovering, J. Bikker and C. Humblet, *J. Med. Chem.*, 2009, **52**, 6752–6756.

10 T. J. Ritchie and S. J. F. MacDonald, *Drug Discovery Today*, 2009, **14**, 1011–1020.

11 T. J. Ritchie, S. J. F. Macdonald, R. J. Young and S. D. Pickett, *Drug Discovery Today*, 2011, **16**, 164–171.

12 T. T. Talele, *J. Med. Chem.*, 2016, **59**, 8712–8756.

13 S. S. Girija, *Mini-Rev. Med. Chem.*, 2016, **16**, 892–904.

14 A. R. Gomes, C. L. Varela, E. J. Tavares-da-Silva and F. M. F. Roleira, *Eur. J. Med. Chem.*, 2020, **201**, 112327.

15 A. Kamath and I. Ojima, *Tetrahedron*, 2012, **68**, 10640–10664.

16 G. Veinberg, I. Potorocina and M. Vorona, *Curr. Med. Chem.*, 2014, **21**, 393–416.

17 J. F. Fisher and S. Mobashery, *The β-lactam (azetidin-2-one) as a privileged ring in medicinal chemistry*, RSC Publishing, 2016.

18 R. I. Storer, C. Aciro and L. H. Jones, *Chem. Soc. Rev.*, 2011, **40**, 2330–2346.

19 L. A. Marchetti, L. K. Kumawat, N. Mao, J. C. Stephens and R. B. P. Elmes, *Chem*, 2019, **5**, 1398–1485.

20 J. R. Hill and A. A. B. Robertson, *J. Med. Chem.*, 2018, **61**, 6945–6963.

21 M. M. Hassan and O. O. Olaoye, *Molecules*, 2020, **25**, 2285.

22 M. W. Halloran and J.-P. Lumb, *Chem. – Eur. J.*, 2019, **25**, 4885–4898.

23 S. Searles, M. Tamres, F. Block and L. A. Quarterman, *J. Am. Chem. Soc.*, 1956, **78**, 4917–4920.

24 RDkit: Open-source chemiinformatics:, http://www.rdkit.org, (accessed Sept 2020).

25 TIBCO Spotfire 10.3.1., https://www.tibco.com/products/tibco-spotfire, (accessed Sept 2020).

26 COSMOtherm release 19.0.1, COSMOlogic GmbH & Co KG, a Dassault Systèmes Company.

27 F. Eckert and A. Klamt, *AIChE J.*, 2002, **48**, 369–385.

28 Integrity, https://integrity.clarivate.com/integrity/xmlxsl/pk_home.util_home, (accessed Aug 2020).

29 A. Gagnon, M. Duplessis and L. Fader, *Org. Prep. Proced. Int.*, 2010, **42**, 1–69.

30 M. L. Landry and J. J. Crawford, *ACS Med. Chem. Lett.*, 2020, **11**, 72–76.

31 A. C. Lai and C. M. Crews, *Nat. Rev. Drug Discovery*, 2017, **16**, 101–114.

32 M. Zengerle, K.-H. Chan and A. Ciulli, *ACS Chem. Biol.*, 2015, **10**, 1770–1777.

33 P. Soares, M. S. Gadd, J. Frost, C. Galdeano, L. Ellis, O. Epemolu, S. Rocha, K. D. Read and A. Ciulli, *J. Med. Chem.*, 2018, **61**, 599–618.

34 S. D. Edmondson, B. Yang and C. Fallan, *Bioorg. Med. Chem. Lett.*, 2019, **29**, 1555–1564.

35 W. Farnaby, M. Koegl, M. J. Roy, C. Whitworth, E. Diers, N. Trainor, D. Zollman, S. Steurer, J. Karolyi-Oezguer, C. Riedmueller, T. Gmaschitz, J. Wachter, C. Dank, M. Galant, B. Sharps, K. Rumpel, E. Traxler, T. Gerstberger, R. Schnitzer, O. Petermann, P. Greb, H. Weinstabl, G. Bader, A. Zoephel, A. Weiss-Puxbaum, K. Ehrenhöfer-Wölfer, S. Wöhrle, G. Boehmelt, J. Rinnenthal, H. Arnhof, N. Wiechens, M.-Y. Wu, T. Owen-Hughes, P. Ettmayer, M. Pearson, D. B. McConnell and A. Ciulli, *Nat. Chem. Biol.*, 2019, **15**, 672–680.

36 C. Hao, F. Zhao, H. Song, J. Guo, X. Li, X. Jiang, R. Huan, S. Song, Q. Zhang, R. Wang, K. Wang, Y. Pang, T. Liu, T. Lu, W. Huang, J. Wang, B. Lin, Z. He, H. Li, F. Li, D. Zhao and M. Cheng, *J. Med. Chem.*, 2018, **61**, 265–285.

37 G. Ouvry, N. Atrux-Tallau, F. Bihl, A. Bondu, C. Bouix-Peter, I. Carlavan, O. Christin, M.-J. Cuadrado, C. Defoin-Platel, S. Deret, D. Duvert, C. Feret, M. Forissier, J.-F. Fournier, D. Froude, F. Hacini-Rachinel, C. S. Harris, C. Hervouet, H. Huguet, G. Lafitte, A.-P. Luzy, B. Musicki, D. Orfila, B. Ozello, C. Pascau, J. Pascau, V. Parnet, G. Peluchon, R. Pierre, D. Piwnica, C. Raffin, P. Rossio, D. Spiesse, N. Taquet, E. Thoreau, R. Vatinel, E. Vial and L. F. Hennequin, *ChemMedChem*, 2018, **13**, 321–337.

38 G. Schwertz, M. C. Witschel, M. Rottmann, R. Bonnert, U. Leartsakulpanich, P. Chitnumsub, A. Jaruwat, W. Ittarat, A. Schäfer, R. A. Aponte, S. A. Charman, K. L. White, A. Kundu, S. Sadhukhan, M. Lloyd, G. M. Freiberg, M. Srikumaran, M. Siggel, A. Zwyssig, P. Chaiyen and F. Diederich, *J. Med. Chem.*, 2017, **60**, 4840–4860.

39 J. J. Crawford, A. R. Johnson, D. L. Misner, L. D. Belmont, G. Castanedo, R. Choy, M. Coraggio, L. Dong, C. Eigenbrot, R. Erickson, N. Ghilardi, J. Hau, A. Katewa, P. B. Kohli, W. Lee, J. W. Lubach, B. S. McKenzie, D. F. Ortwine, L. Schutt, S. Tay, B. Wei, K. Reif, L. Liu, H. Wong and W. B. Young, *J. Med. Chem.*, 2018, **61**, 2227–2245.

40 A. S. Kalgutkar, *J. Med. Chem.*, 2020, **63**, 6276–6302.

41 J. J. Crawford, W. Lee, A. R. Johnson, K. J. Delatorre, J. Chen, C. Eigenbrot, J. Heidmann, S. Kakiuchi-Kiyota, A. Katewa, J. R. Kiefer, L. Liu, J. W. Lubach, D. Misner, H. Purkey, K. Reif, J. Vogt, H. Wong, C. Yu and W. B. Young, *ACS Med. Chem. Lett.*, 2020, **11**, 1588–1597.

42 M. Rappas, A. A. E. Ali, K. A. Bennett, J. D. Brown, S. J. Bucknell, M. Congreve, R. M. Cooke, G. Cseke, C. de Graaf, A. S. Doré, J. C. Errey, A. Jazayeri, F. H. Marshall, J. S.

Mason, R. Mould, J. C. Patel, B. G. Tehan, M. Weir and J. A. Christopher, *J. Med. Chem.*, 2020, **63**, 1528–1543.

43 A. B. Forster, P. Abeywickrema, J. Bunda, C. D. Cox, T. D. Cabalu, M. Egbertson, J. Fay, K. Getty, D. Hall, M. Kornienko, J. Lu, G. Parthasarathy, J. Reid, S. Sharma, W. D. Shipe, S. M. Smith, S. Soisson, S. J. Stachel, H.-P. Su, D. Wang and R. Berger, *Bioorg. Med. Chem. Lett.*, 2017, **27**, 5167–5171.

44 A. K. Ghose, V. N. Viswanadhan and J. J. Wendoloski, *J. Phys. Chem. A*, 1998, **102**, 3762–3772.

45 T. W. Johnson, R. A. Gallego and M. P. Edwards, *J. Med. Chem.*, 2018, **61**, 6401–6420.

46 P. D. Leeson and B. Springthorpe, *Nat. Rev. Drug Discovery*, 2007, **6**, 881–890.

47 H. Hobbs, G. Bravi, I. Campbell, M. Convery, H. Davies, G. Inglis, S. Pal, S. Peace, J. Redmond and D. Summers, *J. Med. Chem.*, 2019, **62**, 6972–6984.

48 W. Zhu, C. Sun, S. Xu, C. Wu, J. Wu, M. Xu, H. Zhao, L. Chen, W. Zeng and P. Zheng, *Bioorg. Med. Chem. Lett.*, 2014, **22**, 6746–6754.

49 K. K. C. Liu, S. Bailey, D. M. Dinh, H. Lam, C. Li, P. A. Wells, M.-J. Yin and A. Zou, *Bioorg. Med. Chem. Lett.*, 2012, **22**, 5114–5117.

50 A. Zask, J. Kaplan, J. C. Verheijen, D. J. Richard, K. Curran, N. Brooijmans, E. M. Bennett, L. Toral-Barza, I. Hollander, S. Ayral-Kaloustian and K. Yu, *J. Med. Chem.*, 2009, **52**, 7942–7945.

51 K. Valkó, C. Bevan and D. Reynolds, *Anal. Chem.*, 1997, **69**, 2022–2029.

52 M. Pettersson, D. S. Johnson, D. A. Rankic, G. W. Kauffman, C. W. Am Ende, T. W. Butler, B. Boscoe, E. Evrard, C. J. Helal, J. M. Humphrey, A. F. Stepan, C. M. Stiff, E. Yang, L. Xie, K. R. Bales, E. Hajos-Korcsok, S. Jenkinson, B. Pettersen, L. R. Pustilnik, D. S. Ramirez, S. J. Steyn, K. M. Wood and P. R. Verhoest, *MedChemComm*, 2017, **8**, 730–743.

53 O. Bezençon, B. Heidmann, R. Siegrist, S. Stamm, S. Richard, D. Pozzi, O. Corminboeuf, C. Roch, M. Kessler, E. A. Ertel, I. Reymond, T. Pfeifer, R. de Kanter, M. Toeroek-Schafroth, L. G. Moccia, J. Mawet, R. Moon, M. Rey, B. Capeleto and E. Fournier, *J. Med. Chem.*, 2017, **60**, 9769–9789.

54 D. Barnes-Seeman, M. Jain, L. Bell, S. Ferreira, S. Cohen, X.-H. Chen, J. Amin, B. Snodgrass and P. Hatsis, *ACS Med. Chem. Lett.*, 2013, **4**, 514–516.

55 A. S. Kalgutkar and J. R. Soglia, *Expert Opin. Drug Metab. Toxicol.*, 2005, **1**, 91–142.

56 H. Gaweska and P. F. Fitzpatrick, *Biomol. Concepts*, 2011, **2**, 365–377.

57 M. A. Cerny and R. P. Hanzlik, *Arch. Biochem. Biophys.*, 2005, **436**, 265–275.

58 D. J. Mitchell, D. Nikolic, R. B. van Breemen and R. B. Silverman, *Bioorg. Med. Chem. Lett.*, 2001, **11**, 1757–1760.

59 Q. Sun, R. Zhu, F. W. Foss and T. L. Macdonald, *Bioorg. Med. Chem. Lett.*, 2007, **17**, 6682–6686.

60 X. Zhuo, Y.-Z. Wang, K.-S. Yeung, J. Zhu, X. S. Huang, K. E. Parcella, K. J. Eastman, J. F. Kadow, N. A. Meanwell, Y.-Z. Shu and B. M. Johnson, *Xenobiotica*, 2018, **48**, 1215–1226.

61 J. P. Driscoll, C. M. Sadlowski, N. R. Shah and A. Feula, *J. Med. Chem.*, 2020, **63**, 6303–6314.

62 J. M. Campbell, M. Lee, J. Clawson, S. Kennedy-Gabb, S. Bethune, A. Janiga, L. Kindon and K. P. Leach, *J. Pharm. Sci.*, 2019, **108**, 2858–2864.

63 M. Darnell and L. Weidolf, *Chem. Res. Toxicol.*, 2013, **26**, 1139–1155.

64 R. G. Ulrich, J. A. Bacon, E. P. Brass, C. T. Cramer, D. K. Petrella and E. L. Sun, *Chem.-Biol. Interact.*, 2001, **134**, 251–270.

65 J. C. Namyslo and D. E. Kaufmann, *Chem. Rev.*, 2003, **103**, 1485–1537.

66 Y. Xu, M. L. Conner and M. K. Brown, *Angew. Chem., Int. Ed.*, 2015, **54**, 11918–11928.

67 S. Poplata, A. Tröster, Y.-Q. Zou and T. Bach, *Chem. Rev.*, 2016, **116**, 9748–9815.

68 K. B. Wiberg, Z. Rappoport and J. F. Liebman, in *The Chemistry of Cyclobutanes*, John Wiley and Sons Inc, 2005.

69 U. R. Anumala, J. Waaler, Y. Nkizinkiko, A. Ignatev, K. Lazarow, P. Lindemann, P. A. Olsen, S. Murthy, E. Obaji, A. G. Majouga, S. Leonov, J. P. von Kries, L. Lehtio, S. Krauss and M. Nazare, *J. Med. Chem.*, 2017, **60**, 10013–10025.

70 K. G. Liu, J. I. Kim, K. Olszewski, A. M. Barsotti, K. Morris, C. Lamarque, X. Yu, J. Gaffney, X. J. Feng, J. P. Patel and M. V. Poyurovsky, *J. Med. Chem.*, 2020, **63**, 5201–5211.

71 M. Kono, A. Ochida, T. Oda, T. Imada, Y. Banno, N. Taya, S. Masada, T. Kawamoto, K. Yonemori, Y. Nara, Y. Fukase, T. Yukawa, H. Tokuhara, R. Skene, B. C. Sang, I. D. Hoffman, G. P. Snell, K. Uga, A. Shibata, K. Igaki, Y. Nakamura, H. Nakagawa, N. Tsuchimori, M. Yamasaki, J. Shirai and S. Yamamoto, *J. Med. Chem.*, 2018, **61**, 2973–2988.

72 M. Kono, T. Oda, M. Tawada, T. Imada, Y. Banno, N. Taya, T. Kawamoto, H. Tokuhara, Y. Tomata, N. Ishii, A. Ochida, Y. Fukase, T. Yukawa, S. Fukumoto, H. Watanabe, K. Uga, A. Shibata, H. Nakagawa, M. Shirasaki, Y. Fujitani, M. Yamasaki, J. Shirai and S. Yamamoto, *Bioorg. Med. Chem. Lett.*, 2018, **26**, 470–482.

73 Y. Zhao, S. Yu, W. Sun, L. Liu, J. Lu, D. McEachern, S. Shargary, D. Bernard, X. Li, T. Zhao, P. Zou, D. Sun and S. Wang, *J. Med. Chem.*, 2013, **56**, 5553–5561.

74 M. L. Vazquez, N. Kaila, J. W. Strohbach, J. D. Trzupek, M. F. Brown, M. E. Flanagan, M. J. Mitton-Fry, T. A. Johnson, R. E. TenBrink, E. P. Arnold, A. Basak, S. E. Heasley, S. Kwon, J. Langille, M. D. Parikh, S. H. Griffin, J. M. Casavant, B. A. Duclos, A. E. Fenwick, T. M. Harris, S. Han, N. Caspers, M. E. Dowty, X. Yang, M. E. Banker, M. Hegen, P. T. Symanowicz, L. Li, L. Wang, T. H. Lin, J. Jussif, J. D. Clark, J. B. Telliez, R. P. Robinson and R. Unwalla, *J. Med. Chem.*, 2018, **61**, 1130–1152.

75 S. P. Nikas, S. O. Alapafuja, I. Papanastasiou, C. A. Paronis, V. G. Shukla, D. P. Papahatjis, A. L. Bowman, A.

Halikhedkar, X. Han and A. Makriyannis, *J. Med. Chem.*, 2010, **53**, 6996–7010.

76 J. M. Lapierre, S. Eathiraj, D. Vensel, Y. Liu, C. O. Bull, S. Cornell-Kennon, S. Iimura, E. W. Kelleher, D. E. Kizer, S. Koerner, S. Makhija, A. Matsuda, M. Moussa, N. Namdev, R. E. Savage, J. Szwaya, E. Volckova, N. Westlund, H. Wu and B. Schwartz, *J. Med. Chem.*, 2016, **59**, 6455–6469.

77 A. Åstrand, A. Töreskog, S. Watanabe, R. Kronstrand, H. Gréen and S. Vikingsson, *Arch. Toxicol.*, 2019, **93**, 95–106.

78 G. B. Quistad, L. E. Staiger and D. A. Schooley, *Drug Metab. Dispos.*, 1986, **14**, 521–525.

79 J. Li, K. Gao, M. Bian and H. Ding, *Org. Chem. Front.*, 2020, **7**, 136–154.

80 J. A. Bull, R. A. Croft, O. A. Davis, R. Doran and K. F. Morgan, *Chem. Rev.*, 2016, **116**, 12150–12233.

81 E. M. Carreira and T. C. Fessard, *Chem. Rev.*, 2014, **114**, 8257–8322.

82 G. Wuitschik, M. Rogers-Evans, K. Muller, H. Fischer, B. Wagner, F. Schuler, L. Polonchuk and E. M. Carreira, *Angew. Chem., Int. Ed.*, 2006, **45**, 7736–7739.

83 J. A. Burkhard, G. Wuitschik, M. Rogers-Evans, K. Muller and E. M. Carreira, *Angew. Chem., Int. Ed.*, 2010, **49**, 9052–9067.

84 M. Berthelot, F. Besseau and C. Laurence, *Eur. J. Org. Chem.*, 1998, 925–931.

85 J. E. Dowling, M. Alimzhanov, L. Bao, M. H. Block, C. Chuaqui, E. L. Cooke, C. R. Denz, A. Hird, S. Huang, N. A. Larsen, B. Peng, T. W. Pontz, C. Rivard-Costa, J. C. Saeh, K. Thakur, Q. Ye, T. Zhang and P. D. Lyne, *ACS Med. Chem. Lett.*, 2013, **4**, 800–805.

86 C. White, M. A. McGowan, H. Zhou, N. Sciammetta, X. Fradera, J. Lim, E. M. Joshi, C. Andrews, E. B. Nickbarg, P. Cowley, S. Trewick, M. Augustin, K. von Köenig, C. A. Lesburg, K. Otte, I. Knemeyer, H. Woo, W. Yu, M. Cheng, P. Spacciapoli, P. Geda, X. Song, N. Smotrov, P. Curran, M. R. Heo, P. Abeywickrema, J. R. Miller, D. J. Bennett and Y. Han, *ACS Med. Chem. Lett.*, 2020, **11**, 550–557.

87 P. N. Collier, H. C. Twin, R. M. A. Knegtel, D. Boyall, G. Brenchley, C. J. Davis, S. Keily, C. Mak, A. Miller, F. Pierard, L. Settimo, C. M. Bolton, P. Chiu, A. Curnock, E. Doyle, A. J. Tanner and J. M. Jimenez, *ACS Med. Chem. Lett.*, 2019, **10**, 1134–1139.

88 X. Zheng, C. Liang, L. Wang, B. Wang, Y. Liu, S. Feng, J. Z. Wu, L. Gao, L. Feng, L. Chen, T. Guo, H. C. Shen and H. Yun, *J. Med. Chem.*, 2018, **61**, 10228–10241.

89 S. Patel, S. F. Harris, P. Gibbons, G. Deshmukh, A. Gustafson, T. Kellar, H. Lin, X. Liu, Y. Liu, Y. Liu, C. Ma, K. Scearce-Levie, A. S. Ghosh, Y. G. Shin, H. Solanoy, J. Wang, B. Wang, J. Yin, M. Siu and J. W. Lewcock, *J. Med. Chem.*, 2015, **58**, 8182–8199.

90 ACD/logD, version 2020.1.2, Advanced Chemistry Development, Inc., Toronto, ON, Canada, www.acdlabs.com, 2020.

91 M. Rogers-Evans, H. Knust, J. M. Plancher, E. M. Carreira, G. Wuitschik, J. Burkhard, D. B. Li and C. Guerot, *Chimia*, 2014, **68**, 492–499.

92 G. Wuitschik, M. Rogers-Evans, A. Buckl, M. Bernasconi, M. Marki, T. Godel, H. Fischer, B. Wagner, I. Parrilla, F. Schuler, J. Schneider, A. Alker, W. B. Schweizer, K. Muller and E. M. Carreira, *Angew. Chem., Int. Ed.*, 2008, **47**, 4512–4515.

93 R. A. Croft, J. J. Mousseau, C. Choi and J. A. Bull, *Chem. – Eur. J.*, 2018, **24**, 818–821.

94 P. Lassalas, K. Oukoloff, V. Makani, M. James, V. Tran, Y. Yao, L. Huang, K. Vijayendran, L. Monti, J. Q. Trojanowski, V. M. Lee, M. C. Kozlowski, A. B. Smith, 3rd, K. R. Brunden and C. Ballatore, *ACS Med. Chem. Lett.*, 2017, **8**, 864–868.

95 J. A. Burkhard, G. Wuitschik, J.-M. Plancher, M. Rogers-Evans and E. M. Carreira, *Org. Lett.*, 2013, **15**, 4312–4315.

96 N. H. Powell, G. J. Clarkson, R. Notman, P. Raubo, N. G. Martin and M. Shipman, *Chem. Commun.*, 2014, **50**, 8797–8800.

97 P. Mukherjee, M. Pettersson, J. K. Dutra, L. Xie and C. W. Am Ende, *ChemMedChem*, 2017, **12**, 1574–1577.

98 X. Q. Li, M. A. Hayes, G. Gronberg, K. Berggren, N. Castagnoli, Jr. and L. Weidolf, *Drug Metab. Dispos.*, 2016, **44**, 1341–1348.

99 F. Toselli, M. Fredenwall, P. Svensson, X. Q. Li, A. Johansson, L. Weidolf and M. A. Hayes, *Drug Metab. Dispos.*, 2017, **45**, 966–973.

100 F. Toselli, M. Fredenwall, P. Svensson, X. Q. Li, A. Johansson, L. Weidolf and M. A. Hayes, *J. Med. Chem.*, 2019, **62**, 7383–7399.

101 P. S. Charifson and W. P. Walters, *J. Med. Chem.*, 2014, **57**, 9701–9717.

102 D. T. Manallack, R. J. Prankerd, E. Yuriev, T. I. Oprea and D. K. Chalmers, *Chem. Soc. Rev.*, 2013, **42**, 485–496.

103 E. Vitaku, D. T. Smith and J. T. Njardarson, *J. Med. Chem.*, 2014, **57**, 10257–10274.

104 G. S. Singh, in *Adv. Heterocycl. Chem.*, ed. E. F. V. Scriven and C. A. Ramsden, Academic Press, 2020, vol. 130, pp. 1–74.

105 V. Mehra, I. Lumb, A. Anand and V. Kumar, *RSC Adv.*, 2017, **7**, 45763–45783.

106 A. Brandi, S. Cicchi and F. M. Cordero, *Chem. Rev.*, 2008, **108**, 3988–4035.

107 H. D. Banks, *J. Org. Chem.*, 2006, **71**, 8089–8097.

108 T. Dudev and C. Lim, *J. Am. Chem. Soc.*, 1998, **120**, 4450–4458.

109 J. B. Lambert, W. L. Oliver and B. S. Packard, *J. Am. Chem. Soc.*, 1971, **93**, 933–937.

110 A. Brown, T. B. Brown, A. Calabrese, D. Ellis, N. Puhalo, M. Ralph and L. Watson, *Bioorg. Med. Chem. Lett.*, 2010, **20**, 516–520.

111 A. Johansson, C. Löfberg, M. Antonsson, S. von Unge, M. A. Hayes, R. Judkins, K. Ploj, L. Benthem, D. Lindén, P. Brodin, M. Wennerberg, M. Fredenwall, L. Li, J. Persson, R. Bergman, A. Pettersen, P. Gennemark and A. Hogner, *J. Med. Chem.*, 2016, **59**, 2497–2511.

112 A. I. de Lucas, J. A. Vega, E. Matesanz, M. L. Linares, A. García Molina, G. Tresadern, H. Lavreysen, A. A. Trabanco and J. M. Cid, *ACS Med. Chem. Lett.*, 2020, **11**, 303–308.

113 R. S. Obach, E. A. LaChapelle, M. A. Brodney, M. Vanase-Frawley, G. W. Kauffman and A. Sawant-Basak, *Xenobiotica*, 2016, **46**, 1112–1121.

114 H. Jia, G. Dai, W. Su, K. Xiao, J. Weng, Z. Zhang, Q. Wang, T. Yuan, F. Shi, Z. Zhang, W. Chen, Y. Sai, J. Wang, X. Li, Y. Cai, J. Yu, P. Ren, J. Venable, T. Rao, J. P. Edwards and S. D. Bembenek, *J. Med. Chem.*, 2019, **62**, 4936–4948.

115 E. R. Hickey, R. Zindell, P. F. Cirillo, L. Wu, M. Ermann, A. K. Berry, D. S. Thomson, C. Albrecht, M. J. Gemkow and D. Riether, *Bioorg. Med. Chem. Lett.*, 2015, **25**, 575–580.

116 L. Kvaernø, M. Werder, H. Hauser and E. M. Carreira, *J. Med. Chem.*, 2005, **48**, 6035–6053.

117 M. Packiarajan, C. G. Ferreira, S. P. Hong, A. D. White, G. Chandrasena, X. Pu, R. M. Brodbeck and A. J. Robichaud, *Bioorg. Med. Chem. Lett.*, 2012, **22**, 6469–6474.

118 S. Cramp, H. J. Dyke, C. Higgs, D. E. Clark, M. Gill, P. Savy, N. Jennings, S. Price, P. M. Lockey, D. Norman, S. Porres, F. Wilson, A. Jones, N. Ramsden, R. Mangano, D. Leggate, M. Andersson and R. Hale, *Bioorg. Med. Chem. Lett.*, 2010, **20**, 2516–2519.

119 D. S. Palacios, E. L. Meredith, T. Kawanami, C. M. Adams, X. Chen, V. Darsigny, M. Palermo, D. Baird, E. L. George, C. Guy, J. Hewett, L. Tierney, S. Thigale, L. Wang and W. A. Weihofen, *ACS Med. Chem. Lett.*, 2019, **10**, 1524–1529.

120 D. Gustafsson, R. Bylund, T. Antonsson, I. Nilsson, J. E. Nyström, U. Eriksson, U. Bredberg and A. C. Teger-Nilsson, *Nat. Rev. Drug Discovery*, 2004, **3**, 649–659.

121 R. M. Rzasa, M. J. Frohn, K. L. Andrews, S. Chmait, N. Chen, J. G. Clarine, C. Davis, H. A. Eastwood, D. B. Horne, E. Hu, A. D. Jones, M. R. Kaller, R. K. Kunz, S. Miller, H. Monenschein, T. Nguyen, A. J. Pickrell, A. Porter, A. Reichelt, X. Zhao, J. J. S. Treanor and J. R. Allen, *Bioorg. Med. Chem.*, 2014, **22**, 6570–6585.

122 R. M. Rzasa, E. Hu, S. Rumfelt, N. Chen, K. L. Andrews, S. Chmait, J. R. Falsey, W. Zhong, A. D. Jones, A. Porter, S. W. Louie, X. Zhao, J. J. Treanor and J. R. Allen, *Bioorg. Med. Chem. Lett.*, 2012, **22**, 7371–7375.

123 J. Allen, D. B. Horne, E. Hu, M. R. Kaller, H. Monenschein, T. T. Nguyen, A. Reichelt and R. M. Rzasa, WO2011143495A1, Amgen Inc., USA, 2011.

124 A. Sawant-Basak, K. J. Coffman, G. S. Walker, T. F. Ryder, E. Tseng, E. Miller, C. Lee, M. A. Vanase-Frawley, J. W. Wong, M. A. Brodney, T. Rapp and R. S. Obach, *J. Pharm. Sci.*, 2013, **102**, 3277–3293.

125 J. Bolleddula, K. DeMent, J. P. Driscoll, P. Worboys, P. J. Brassil and D. L. Bourdet, *Drug Metab. Rev.*, 2014, **46**, 379–419.

126 H. Kurata, K. Kusumi, K. Otsuki, R. Suzuki, M. Kurono, Y. Takada, H. Shioya, T. Komiya, H. Mizuno, T. Ono, H. Hagiya, M. Minami, S. Nakade and H. Habashita, *Bioorg. Med. Chem. Lett.*, 2011, **21**, 3885–3889.

127 A. J. Dyckman, *J. Med. Chem.*, 2017, **60**, 5267–5289.

128 J. J. Hale, C. L. Lynch, W. Neway, S. G. Mills, R. Hajdu, C. A. Keohane, M. J. Rosenbach, J. A. Milligan, G.-J. Shei, S. A. Parent, G. Chrebet, J. Bergstrom, D. Card, M. Ferrer, P. Hodder, B. Strulovici, H. Rosen and S. Mandala, *J. Med. Chem.*, 2004, **47**, 6662–6665.

129 N. Kaplan, M. Albert, D. Awrey, E. Bardouniotis, J. Berman, T. Clarke, M. Dorsey, B. Hafkin, J. Ramnauth, V. Romanov, M. B. Schmid, R. Thalakada, J. Yethon and H. W. Pauls, *Antimicrob. Agents Chemother.*, 2012, **56**, 5865–5874.

130 M. Takhi, K. Sreenivas, C. K. Reddy, M. Munikumar, K. Praveena, P. Sudheer, B. N. Rao, G. Ramakanth, J. Sivaranjani, S. Mulik, Y. R. Reddy, K. Narasimha Rao, R. Pallavi, A. Lakshminarasimhan, S. K. Panigrahi, T. Antony, I. Abdullah, Y. K. Lee, M. Ramachandra, R. Yusof, N. A. Rahman and H. Subramanya, *Eur. J. Med. Chem.*, 2014, **84**, 382–394.

131 For related examples on the effect on metabolic stability when moving from a dimethylamine to an azetidine substituent on an aromatic ring, see: (*a*) M. P. Alam, O. M. Khdour, P. M. Arce, Y. Chen, B. Roy, W. G. Johnson, S. Dey and S. M. Hecht, *Bioorg. Med. Chem.*, 2014, **22**, 4935–4947; (*b*) J. L. Henderson, B. L. Kormos, M. M. Hayward, K. J. Coffman, J. Jasti, R. G. Kurumbail, T. T. Wager, P. R. Verhoest, G. S. Noell, Y. Chen, E. Needle, Z. Berger, S. J. Steyn, C. Houle, W. D. Hirst and P. Galatsis, *J. Med. Chem.*, 2015, **58**, 419–432.

132 C. M. Tice, Y. Zheng and S. B. Singh, in *Comprehensive Medicinal Chemistry III*, ed. S. Chackalamannil, D. Rotella and S. E. Ward, Elsevier, Oxford, 2017, pp. 211–263.

133 A. A. Kirichok, I. Shton, M. Kliachyna, I. Pishel and P. K. Mykhailiuk, *Angew. Chem., Int. Ed.*, 2017, **56**, 8865–8869.

134 A. A. Kirichok, I. O. Shton, I. M. Pishel, S. A. Zozulya, P. O. Borysko, V. Kubyshkin, O. A. Zaporozhets, A. A. Tolmachev and P. K. Mykhailiuk, *Chem. – Eur. J.*, 2018, **24**, 5444–5449.

135 I. Churcher, *J. Med. Chem.*, 2018, **61**, 444–452.

136 L. M. Luh, U. Scheib, K. Juenemann, L. Wortmann, M. Brands and P. M. Cromm, *Angew. Chem., Int. Ed.*, 2020, **59**, 15448–15466.

137 X. Han, L. Zhao, W. Xiang, C. Qin, B. Miao, T. Xu, M. Wang, C. Y. Yang, K. Chinnaswamy, J. Stuckey and S. Wang, *J. Med. Chem.*, 2019, **62**, 11218–11231.

138 V. Zoppi, S. J. Hughes, C. Maniaci, A. Testa, T. Gmaschitz, C. Wieshofer, M. Koegl, K. M. Riching, D. L. Daniels, A. Spallarossa and A. Ciulli, *J. Med. Chem.*, 2019, **62**, 699–726.

139 D. W. Robbins, A. T. Sands, J. McIntosh, J. Mihalic, J. Wu, D. Kato, D. Weiss and G. Peng, WO2020081450A1, Nurix Therapeutics, Inc., USA, 2020.

140 A. P. Crew, Y. Qian, H. Dong, J. Wang, K. R. Hornberger and C. M. Crews, WO2018102725A1, Arvinas, Inc., USA, 2018.

141 K. P. McCusker and D. G. Fujimori, *ACS Chem. Biol.*, 2012, **7**, 64–72.

142 P. Fernandes, D. Pereira, P. B. Watkins and D. Bertrand, *J. Med. Chem.*, 2020, **63**, 6462–6473.

143 T. V. Magee, S. L. Ripp, B. Li, R. A. Buzon, L. Chupak, T. J. Dougherty, S. M. Finegan, D. Girard, A. E. Hagen, M. J. Falcone, K. A. Farley, K. Granskog, J. R. Hardink, M. D. Huband, B. J. Kamicker, T. Kaneko, M. J. Knickerbocker, J. L. Liras, A. Marra, I. Medina, T. T. Nguyen, M. C. Noe,

R. S. Obach, J. P. O'Donnell, J. B. Penzien, U. D. Reilly, J. R. Schafer, Y. Shen, G. G. Stone, T. J. Strelevitz, J. Sun, A. Tait-Kamradt, A. D. Vaz, D. A. Whipple, D. W. Widlicka, D. G. Wishka, J. P. Wolkowski and M. E. Flanagan, *J. Med. Chem.*, 2009, **52**, 7446–7457.

144 N. De Rycke, O. David and F. Couty, *Org. Lett.*, 2011, **13**, 1836–1839.

145 P. Hopes, T. Langer, K. Millard and A. Steven, *Org. Process Res. Dev.*, 2018, **22**, 996–1006.

146 J. K. Lynch, M. W. Holladay, K. B. Ryther, H. Bai, C.-N. Hsiao, H. E. Morton, D. A. Dickman, W. Arnold and S. A. King, *Tetrahedron: Asymmetry*, 1998, **9**, 2791–2794.

147 H. K. Zhang, L. F. Yu, J. B. Eaton, P. Whiteaker, O. K. Onajole, T. Hanania, D. Brunner, R. J. Lukas and A. P. Kozikowski, *J. Med. Chem.*, 2013, **56**, 5495–5504.

148 M. M. Claffey, C. J. Helal, P. R. Verhoest, Z. Kang, K. S. Fors, S. Jung, J. Zhong, M. W. Bundesmann, X. Hou, S. Lui, R. J. Kleiman, M. Vanase-Frawley, A. W. Schmidt, F. Menniti, C. J. Schmidt, W. E. Hoffman, M. Hajos, L. McDowell, R. E. O'Connor, M. Macdougall-Murphy, K. R. Fonseca, S. L. Becker, F. R. Nelson and S. Liras, *J. Med. Chem.*, 2012, **55**, 9055–9068.

149 X.-Q. Li, G. Grönberg, E.-H. Bangur, M. A. Hayes, N. Castagnoli and L. Weidolf, *Drug Metab. Dispos.*, 2019, **47**, 1247–1256.

150 M. P. Patricelli, M. R. Janes, L. S. Li, R. Hansen, U. Peters, L. V. Kessler, Y. Chen, J. M. Kucharski, J. Feng, T. Ely, J. H. Chen, S. J. Firdaus, A. Babbar, P. Ren and Y. Liu, *Cancer Discovery*, 2016, **6**, 316–329.

151 Y. Wang, L. Li, J. Fan, Y. Dai, A. Jiang, M. Geng, J. Ai and W. Duan, *J. Med. Chem.*, 2018, **61**, 9085–9104.

152 P. A. Jackson, J. C. Widen, D. A. Harki and K. M. Brummond, *J. Med. Chem.*, 2017, **60**, 839–885.

153 R. Lonsdale and R. A. Ward, *Chem. Soc. Rev.*, 2018, **47**, 3816–3830.

154 M. D. Palkowitz, B. Tan, H. Hu, K. Roth and R. A. Bauer, *Org. Lett.*, 2017, **19**, 2270–2273.

155 T. Suzuki, J.-i. Kusakabe, K. Kitazawa, T. Nakagawa, S. Kawauchi and T. Ishizone, *Macromolecules*, 2010, **43**, 107–116.

156 D. Angst, F. Gessier, P. Janser, A. Vulpetti, R. Wälchli, C. Beerli, A. Littlewood-Evans, J. Dawson, B. Nuesslein-Hildesheim, G. Wieczorek, S. Gutmann, C. Scheufler, A. Hinniger, A. Zimmerlin, E. G. Funhoff, R. Pulz and B. Cenni, *J. Med. Chem.*, 2020, **63**, 5102–5118.

157 R. Pellicciari, M. Raimondo, M. Marinozzi, B. Natalini, G. Costantino and C. Thomsen, *J. Med. Chem.*, 1996, **39**, 2874–2876.

158 J. Kanazawa and M. Uchiyama, *Synlett*, 2019, **30**, 1–11.

159 M. Kondo, J. Kanazawa, T. Ichikawa, T. Shimokawa, Y. Nagashima, K. Miyamoto and M. Uchiyama, *Angew. Chem., Int. Ed.*, 2020, **59**, 1970–1974.

160 X. Ma, D. L. Sloman, Y. Han and D. J. Bennett, *Org. Lett.*, 2019, **21**, 7199–7203.

161 J. Nugent, C. Arroniz, B. R. Shire, A. J. Sterling, H. D. Pickford, M. L. J. Wong, S. J. Mansfield, D. F. J. Caputo, B.

Owen, J. J. Mousseau, F. Duarte and E. A. Anderson, *ACS Catal.*, 2019, **9**, 9568–9574.

162 J. Nugent, B. R. Shire, D. F. J. Caputo, H. D. Pickford, F. Nightingale, I. T. T. Houlsby, J. J. Mousseau and E. A. Anderson, *Angew. Chem., Int. Ed.*, 2020, **59**, 11866–11870.

163 N. Trongsiriwat, Y. Pu, Y. Nieves-Quinones, R. A. Shelp, M. C. Kozlowski and P. J. Walsh, *Angew. Chem., Int. Ed.*, 2019, **58**, 13416–13420.

164 M. D. VanHeyst, J. Qi, A. J. Roecker, J. M. E. Hughes, L. Cheng, Z. Zhao and J. Yin, *Org. Lett.*, 2020, **22**, 1648–1654.

165 M. L. J. Wong, J. J. Mousseau, S. J. Mansfield and E. A. Anderson, *Org. Lett.*, 2019, **21**, 2408–2411.

166 X. Zhang, R. T. Smith, C. Le, S. J. McCarver, B. T. Shireman, N. I. Carruthers and D. W. C. MacMillan, *Nature*, 2020, **580**, 220–226.

167 I. S. Makarov, C. E. Brocklehurst, K. Karaghiosoff, G. Koch and P. Knochel, *Angew. Chem., Int. Ed.*, 2017, **56**, 12774–12777.

168 M. R. Barbachyn, D. K. Hutchinson, D. S. Toops, R. J. Reid, G. E. Zurenko, B. H. Yagi, R. D. Schaadt and J. W. Allison, *Bioorg. Med. Chem. Lett.*, 1993, **3**, 671–676.

169 G. M. Locke, S. S. R. Bernhard and M. O. Senge, *Chem. – Eur. J.*, 2019, **25**, 4590–4647.

170 A. F. Stepan, C. Subramanyam, I. V. Efremov, J. K. Dutra, T. J. O'Sullivan, K. J. DiRico, W. S. McDonald, A. Won, P. H. Dorff, C. E. Nolan, S. L. Becker, L. R. Pustilnik, D. R. Riddell, G. W. Kauffman, B. L. Kormos, L. Zhang, Y. Lu, S. H. Capetta, M. E. Green, K. Karki, E. Sibley, K. P. Atchison, A. J. Hallgren, C. E. Oborski, A. E. Robshaw, B. Sneed and C. J. O'Donnell, *J. Med. Chem.*, 2012, **55**, 3414–3424.

171 P. K. Mykhailiuk, *Org. Biomol. Chem.*, 2019, **17**, 2839–2849.

172 Y. L. Goh, Y. T. Cui, V. Pendharkar and V. A. Adsool, *ACS Med. Chem. Lett.*, 2017, **8**, 516–520.

173 N. D. Measom, K. D. Down, D. J. Hirst, C. Jamieson, E. S. Manas, V. K. Patel and D. O. Somers, *ACS Med. Chem. Lett.*, 2017, **8**, 43–48.

174 E. G. Tse, S. D. Houston, C. M. Williams, G. P. Savage, L. M. Rendina, I. Hallyburton, M. Anderson, R. Sharma, G. S. Walker, R. S. Obach and M. H. Todd, *J. Med. Chem.*, 2020, **63**, 11585–11601.

175 Q. Pu, H. Zhang, L. Guo, M. Cheng, A. C. Doty, H. Ferguson, X. Fradera, C. A. Lesburg, M. A. McGowan, J. R. Miller, P. Geda, X. Song, K. Otte, N. Sciammetta, N. Solban, W. Yu, D. L. Sloman, H. Zhou, A. Lammens, L. Neumann, D. J. Bennett, A. Pasternak and Y. Han, *ACS Med. Chem. Lett.*, 2020, **11**, 1548–1554.

176 S. D. Nelson, *J. Med. Chem.*, 1982, **25**, 753–765.

177 T. M. Sodano, L. A. Combee and C. R. J. Stephenson, *ACS Med. Chem. Lett.*, 2020, **11**, 1785–1788.

178 K. B. Wiberg, B. S. Ross, J. J. Isbell and N. McMurdie, *J. Org. Chem.*, 1993, **58**, 1372–1376.

179 Y. P. Auberson, C. Brocklehurst, M. Furegati, T. C. Fessard, G. Koch, A. Decker, L. La Vecchia and E. Briard, *ChemMedChem*, 2017, **12**, 590–598.

180   A. Aguilar, J. Lu, L. Liu, D. Du, D. Bernard, D. McEachern, S. Przybranowski, X. Li, R. Luo, B. Wen, D. Sun, H. Wang, J. Wen, G. Wang, Y. Zhai, M. Guo, D. Yang and S. Wang, *J. Med. Chem.*, 2017, **60**, 2819–2839.

181   K. C. Nicolaou, D. Vourloumis, S. Totokotsopoulos, A. Papakyriakou, H. Karsunky, H. Fernando, J. Gavrilyuk, D. Webb and A. F. Stepan, *ChemMedChem*, 2016, **11**, 31–37.

182   R. Nusse, A. Brown, J. Papkoff, P. Scambler, G. Shackleford, A. McMahon, R. Moon and H. Varmus, *Cell*, 1991, **64**, 231.

183   N. T. Thirumoorthi and V. A. Adsool, *Org. Biomol. Chem.*, 2016, **14**, 9485–9489.

184   V. V. Levterov, Y. Panasyuk, V. O. Pivnytska and P. K. Mykhailiuk, *Angew. Chem., Int. Ed.*, 2020, **59**, 7161–7167.

185   R. M. Bychek, V. Hutskalova, Y. P. Bas, O. A. Zaporozhets, S. Zozulya, V. V. Levterov and P. K. Mykhailiuk, *J. Org. Chem.*, 2019, **84**, 15106–15117.

186   J. Zhao, Y. Chang, J. Elleraas, T. P. Montgomery, J. E. Spangler, S. K. Nair, M. Del Bel, G. M. Gallego, J. J. Mousseau, M. A. Perry, M. R. Collins, J. Vantourout and P. Baran, ChemRxiv, 2020, Preprint, DOI: 10.26434/chemrxiv.13120283.v1.

187   N. Rioux, K. W. Duncan, R. J. Lantz, X. Miao, E Chan-Penebre, M. P. Moyer, M. J. Munchhof, R. A. Copeland, R. Chesworth and N. J. Waters, Species differences in metabolism of EPZ015666, an oxetane-containing protein arginine methyltransferase-5 (PRMT5) inhibitor, *Xenobiotica*, 2016, **46**(3), 26294260.